NTNU
Norwegian University of Science and Technology
Department of Marine Technology

M.Sc.THESIS

Title:	**Delivered:**
Clump-weight Trawl Gear Interaction with Submarine Pipelines	05.07.11
	Availability: Open
Student: Krisitan Maalø	**Number of pages:** 87

Abstract:

A recent development in bottom trawling is the use of twin trawl equipment, where two trawl nets are towed side by side from a single vessel. This increases the catch rate and efficiently of the trawler. Governed by cost and catch optimization, the use of twin trawl systems are expected to become more popular in the future. Using two trawl nets will, in addition to trawl doors on each side, require a heavy clump weight in the middle to prevent the trawl nets lifting from the seabed. The largest clump weights can have a mass up to 9000 kg and can cause substantial load towed across subsea pipelines, and may in many cases be the governing design load with respect to external loads in pipeline design.

The main objective in this thesis work was to simulate and investigate pull-over forces from clump weights on free spanning pipelines. All simulations were carried out in the computer software SIMLA. Six different small scale tests were simulated in order to verify the finite element model, a very good agreement was obtained.

Design loads from trawl gear are generally implemented according to DNV-RP-F111. The calculation methods provided in this recommended practice are based on the same small scale tests which was made available to this thesis work for verification purposes. The validity range of DNV-RP-F111 reflects the range of the small scale tests i.e. only valid for rigid pipelines.

The effect of increasing pipeline flexibility was investigated. Simulations were carried out for span heights 0.25m, 0.50m and 0.75m for a 12” pipeline. Two different pipeline models was applied, a 25 m rigid pipeline model with spring representing the lateral pipeline stiffness, and a 1000m pipeline model including realistic soil resistance. The major finding was that pull-over forces decrease for increasing pipeline flexibility. Compared to DNV-RP-F111 the obtained pull-over loads was found considerably lower, both in magnitude and duration. To avoid over-conservatism it is thus recommended that a design method accounting for pipeline flexibility should be developed and used in future pipeline designs.

The effect of warp angle was simulated varying the warp line length from 2.5 to 3.5 times the water depth. The horizontal pull-over force was found to increase for increasing warp line length.

Regarding clump weight design and towing configuration, simulations have shown that a forward clump weight center of gravity will reduce the pull-over loads. Applying a lower warp line attachment point resulted in a more uniform sliding motion of the clump weight during interference and pull-over loads was almost complete reduced to a case of initial impact. It is thus suggested that future clump weight design should reflect this to reduce interference loads on both trawl gear and subsea pipelines

Keyword:

Trawl gear, Clump weight, Pipeline, DNV-RP-F111, SIMLA

Advisor:

Prof. Svein Sævik

Address:
NTNU
Department of Marine Technology
N-7491 Trondheim

Location
Marinteknisk Senter
O. Nielsens vei 10

Tel. +47 73 595501
Fax +47 73 595697

NTNU Trondheim
Norges teknisk-naturvitenskapelige universitet
Institutt for marin teknikk

THESIS WORK SPRING 2011

for

Stud. tech. Kristian Maalø

Clump-weight trawl gear interaction with submarine pipelines

Samvirke mellom klumpvekt trålutstyr og offshore rørledninger

A large network of subsea pipelines have been installed at the Norwegian continental shelf and for large diameter cases (> 16") these are in most cases left exposed on the seabed. The fishing activity in the area is often based on bottom trawl gear, consisting of a trawl net kept open by a trawl door, one at each side of the net. The trawl doors are further pulled by a cable connected to the vessel, the purpose of the doors being to keep the cables separated and the trawl net open. In order to allow for two trawl nets, clump weights connected to a separate pull cable may be applied in the middle. The clump weight mass, including hydrodynamic mass may be more than 10000 kg and when its hits a pipeline, two load effects govern:

1. An initial impact that may damage the coating and cause steel wall denting.
2. A "Pull-over" force which is a more long periodic force needed to pull the trawlboard over the pipeline. This force depending on the several parameters such as the mass, pipe diameter, free span height and length, cable stiffness, soil stiffness etc.

In many cases, item 2 above governs the design with respect to external loads on subsea pipelines, specially for high temperature pipelines.

This master work focus on the pipeline free-span response due to "Pull-over" loads from clump weights and eventual differences between the results obtained from simulating the physical contact behaviour using SIMLA and the results obtained by using the point load-time histories directly as proposed in DnV Recommended Practice DnV-RP-F111. The work is to include:

1) Literature study, including trawling technology, offshore pipeline technology including design loads, failure modes and design criteria, recommended practices for pipeline trawl gear loads and response analysis, non-linear finite element methods with focus on the methods applied in the computer program SIMLA and the thesis work already carried out by M.Sc. Martin Møller and M.Sc. Vegard Longva.
2) Establish analysis scenarios with respect to span length, pipe diameter and mass, warp line length, clump weight design and soil properties including which parameters to be varied. This is to be carried out in cooperation with REINERTSEN.
3) Establish associated SIMLA models for the following scenarios:
   a) Application of point load histories from DnV RP-F111
   b) Clump weight and warp line model with contact elements

4) Perform simulations applying the DnV-RP-F111 models.
5) Perform simulations applying the contact models.
6) Compare the pipeline response quantities.
7) Conclusions and recommendations for further work

The work scope may prove to be larger than initially anticipated. Subject to approval from the supervisors, topics may be deleted from the list above or reduced in extent.

In the thesis the candidate shall present his personal contribution to the resolution of problems within the scope of the thesis work

Theories and conclusions should be based on mathematical derivations and/or logic reasoning identifying the various steps in the deduction.

The candidate should utilise the existing possibilities for obtaining relevant literature.

Thesis format
The thesis should be organised in a rational manner to give a clear exposition of results, assessments, and conclusions. The text should be brief and to the point, with a clear language. Telegraphic language should be avoided.

The thesis shall contain the following elements: A text defining the scope, preface, list of contents, summary, main body of thesis, conclusions with recommendations for further work, list of symbols and acronyms, references and (optional) appendices. All figures, tables and equations shall be numerated.

The supervisors may require that the candidate, in an early stage of the work, presents a written plan for the completion of the work.

The original contribution of the candidate and material taken from other sources shall be clearly defined. Work from other sources shall be properly referenced using an acknowledged referencing system.

The report shall be submitted in three copies:
- Signed by the candidate
- The text defining the scope included
- In bound volume(s)
- Drawings and/or computer prints which cannot be bound should be organised in a separate folder.

Ownership
NTNU has according to the present rules the ownership of the thesis. Any use of the thesis has to be approved by NTNU (or external partner when this applies). The department has the right to use the thesis as if the work was carried out by a NTNU employee, if nothing else has been agreed in advance.

Thesis supervisors
Prof. Svein Sævik
PhD. Hagbart S. Alsos, REINERTSEN

Deadline: 14th June, 2011

Trondheim, Januar 13, 2011

Svein Sævik

Preface

This report is a result of my master thesis specializing in marine structural engineering at Department of Marine Technology, NTNU. The thesis work was carried out during spring semester 2011 in collaboration with Reinertsen AS.

The main object of my master thesis was to simulate trawl loads on subsea pipelines, or more specific application of clump weights, which is a recent development in trawl gear equipment applied in Norwegian Waters. In general, knowledge regarding loads from this type of equipment is scarce and working with this subject have been both inspiring and educational.

A preliminary project is normally carried out as preparation to the master thesis. My preliminary project during autumn 2010 focused on another subject, hence the learning curve has been steep during this thesis work due to familiarizing with a new topic and finite element software. The work load has proven large, considering this and the initial scope of work. Especially developing a SIMLA model was time consuming and challenging.

The focus of the work has to some degree been changed in consultation with my supervisors. According to the initial scope, global pipeline response as a result of induced trawl loads was to be investigated and compared to DNV-RP-F111. However, early in the thesis the induced trawl loads themselves was considered of great interest. Hence, my efforts have mainly been focused on the induced trawl loads and factors with influence the magnitude of the loads, comparing this to DNV-RP-F111.

Enclosed with this report is a DVD containing a digital copy of the report, SIMLA input files for all simulations carried out, in addition to a selection of animations and SIMLA result files (.raf-files).

I would like to express my gratitude to my professor Svein Sævik for excellent guidance, continuous support and encouragement. I would also like to thank PhD. Hagbart Alsos at Reinertsen AS for initially proposing the subject of my thesis, excellent guidance and feedback. In addition, Reinertsen AS should be acknowledged for making their resources available and Statoil for providing the experimental test results used for verification purposes.

.....
Kristian Maalø
July 5, 2011, Trondheim

Contents

List of Figures

List of Tables

List of Symbols

c_s	pipe end damping
C	damping coefficient
C_a	added mass coefficient
C_d	drag coefficient
d	water depth
D_r	diameter of clump weight roller
E	Youngs's modulus
EA	axial stiffness
EI	bending stiffness
F_p	maximum horizontal pull-over force on pipe
F_s	pretensioning of pipe end spring
F_w	warp line force
$F_{w,z}$	warp line vertical force component
F_z	maximum vertical pull-over force on pipe
g	gravitational acceleration
$h^{'}$	dimensionless moment arm, to calculate clump weight pull-over load
H_{sp}	free span height,measured from seabed gap to lowest point of pipeline
k_c	contact stiffness
k_w	warp line stiffness
l	length of structural pipe element
l_{fs}	length of free span
l_{lw}	length of lower part of warp line
l_r	length of clump weight roller
l_s	sweep line length
l_t	total length of clump weight
l_{uw}	length of upper part of warp line
l_w	warp line length

L_{clump}	distance from clump weight center of gravity to reaction point
m	structural mass
m_a	added mass
m_b	mass of clump weight ballast
m_f	mass of clump weight frame
m_r	mass of clump weight roller
m_t	clump weight steel mass
OD	outer pipeline diameter including coating
r_c	clump weight moment arm relative to reaction point
r_w	warp line moment arm relative to reaction point
t_w	Wall thickness of steel pipe
T_p	pull-over duration
V	trawling velocity
w_s	submerged weight
C	system damping matrix
K	system stiffness matrix
M	system mass matrix
α_1, α_2	Rayleigh damping parameters
δ_p	global pipeline deflection at point of trawl pull-over
θ	sweep line angle
λ	damping ratio
ρ	density of seawater
ϕ	warp line angle
ψ	vertical sweep line angle

Chapter 1

Introduction

1.1 Background and Motivation

Subsea pipelines are used for a number of purposes in the offshore petroleum industry, ranging from small diameter pipelines for infield transportation of product, chemicals and injection water, to large diameter export pipelines. Common for all pipelines is the need to insure safe operation and pipeline integrity for all loads which may be anticipated during a life time of operation. This may include environmental loads such as waves and currents, operational loads such as internal pressure and temperature loading and external interference loads such as dropped anchors and fishing activity.

The offshore petroleum industry and fishing industry often operates in the same areas. On the Norwegian continental shelf a large network of subsea pipelines have been installed. The fishing activity in these areas is often based on bottom trawl gear. Regular interaction from these types of gear may be of concern to pipelines laid exposed on the seabed. Both the initial impact and subsequent pull-over loads, i.e. when the trawl gear is pulled over the pipeline, may impose substantial loads to the pipeline.

In Norwegian sector, it is required that all subsea installations shall not unnecessarily or to an unreasonable extent impede or obstruct fishing activities [3]. In addition, subsea installations are known attract fish [3]. Hence future fishing activities cannot be completely disregarded even if the pipeline is routed outside the fishing banks. This requirement, combined with strict design criteria will require robust pipeline designs. Increasing the pipeline resistance towards trawl gear interference can be done by increasing the pipeline steel wall thickness and adding coating. Free spans can be reduced by rock dumping and in some cases a complete burial of the pipeline may be necessary. All of this drives the development cost in pipeline design and especially seabed intervention work is expensive. Thus, for the offshore petroleum industry and future field developments it is of great importance to avoid over-estimation of trawl gear interference loads, leading to unnecessary conservatism in pipeline designs.

Trawl gear design loads are generally implemented according to DNV-RP-F111. This recommended practice was published by DNV (Det Norske Veritas) and aims specifically to provide rational design criteria and guidance on design methods regarding trawl gear interference with subsea pipelines. However, except from the calculation methods provided within DNV-RP-F111, which are mainly based on experimental test, the knowledge of trawl gear interference with pipelines is scarce. From a pipeline designers view, the current engineering practice, applying these calculations methods are believed to over-estimate the trawl gear interference loads.

This thesis work aims to investigate the possibility of performing more detailed calculations regarding trawl gear interference on subsea pipelines and further comparing this to current engineering practice DNV-RP-F111 in order to identify and explain eventual differences such as unnecessary conservatism can be avoided in future pipeline designs.

1.2 Scope of Thesis

Trawl gear pull-over interference has previously been investigated by Martin T. Møller [14] and Vegard Longva [12], successfully applying the finite element software SIMLA in simulation of trawl door interference with pipelines. This thesis work will continue on this work and aim to establish a SIMLA contact model for simulation of clump weight pull-over interference for free spanning pipelines.

According to the initial scope, global pipeline response as a result of clump weight pull-over loads was to be investigated and compared to DNV-RP-F111. However, early in this thesis work the pull-over loads themselves were considered of great interest. Little is known regarding clump weight behavior, magnitude of loading and load shapes during pull-over interference, especially when interacting with flexible pipelines. Hence, this thesis work focuses on investigating the pull-over load and factors which may influence the magnitude of loading, comparing this to DNV-RP-F111.

The duration, and thus load shape of the DNV pull-over design loads needs to be determined in an iterative procedure applying a dynamic finite element analysis. For this purpose a point load model is established in order to calculate the design loads for the different pipeline scenarios considered.

A contact model is developed for simulating the physical clump weight behavior during interference. This model consists of a 1000 m in length pipeline section including, a 50 m free span, realistic soil resistance and pipeline flexibility. From this model, horizontal and vertical pull-over forces and pipeline displacements will be presented as time histories illustrating different load effects and differences compared to DNV-RP-F111.

The small scale experimental tests which form the basis of the calculation methods provided in DNV-RP-F111 have in this thesis work been made available for verification purposes. For this purpose an additional full scale SIMLA model representing the test configuration is developed. This model includes a 25 m pipeline section and lateral pipeline stiffness was represented by springs at each pipe end. Six different test scenarios varying span height and degree of pipeline stiffness are simulated and compared in order to verify the physical clump weight contact model.

The validity range of DNV-RP-F111 reflects the range of the small scale experimental tests i.e. only valid for rigid pipeline configurations. The knowledge of how increased pipeline flexibility could influence the pull-over load is scares, thus simulations are carried out varying lateral pipeline flexibility in order to investigating this effect.

The clump weight design and trawling configuration may be factors which could influence clump weight behavior and magnitude of the pull-over load. Knowledge regarding this may in the future contribute in reducing interference loads to both trawl gear and pipelines. Thus, simulations regarding clump weight center of gravity, warp line attachment point and warp angle is carried out.

In total, three different SIMLA models have been established, a DNV point load model, a contact model including seabed and soil properties, and a contact model consistent with experimental test configuration. Both contact models are modeled with the same trawl gear configuration, which reflects the trawl gear configuration used in the experimental tests. Only a roller type clump weight is considered.

Several assumptions and simplifications have however been made to the SIMLA models, mainly in order to reduce modeling and computational efforts. For instance, the seabed is modeled completely flat in all cases. Local deformation clump weight and denting of the pipeline is disregarded. The 1000 m free spanning pipeline model is developed to provoke a general flexible pipeline response, thus the pipeline is in this case modeled in empty condition, i.e. the without internal pressure and temperature loading. The pipeline will be in tension prior to interference, thus buckling effect due to trawl gear interference is not considered. A linear pipeline material have been regarded as sufficient in all simulation, assuming that eventual local plasticity of the pipeline is of minor importance for the clump weight behavior and magnitude of pull-over loads. Other minor amendments to the SIMLA models is described as they come along in Chapter 4.

1.3 Structure of Thesis

Chapter 2: Gives a short introduction to different bottom trawling concepts in Norwegian Waters and how these types of trawl gear may interact with subsea pipelines. The DNV-RP-F111 calculation method for estimation of clump weights pull-over loads is reviewed. Further, a brief description of the experimental tests are given.

Chapter 3: Presents a short introduction to non-linear effects included in simulating clump weight pull-over interference and the application of SIMLA for this purpose.

Chapter 4: Describes all aspects of modeling in SIMLA, including the trawl gear configuration, clump weight model and the two different pipeline models. A description of seabed interaction, special considerations made to the contact element arrangement and interaction curves are also included. At the end, the general simulations procedure and the sampling method used to extract pull-over forces from the SIMLA are described.

Chapter 5: Contains all of the simulation results which are discussed as they are presented. Pull-over forces and horizontal pipeline displacements are given as time histories. The six simulations carried out to verify the contact model are also presented in detail in this chapter. In addition, the typical clump weight behavior and pipeline response as observed in the simulations are illustrated and commented.

Chapter 6: Final concluding remarks are made regarding the simulation results. Based on this thesis work, recommendations for further work will be given.

Chapter 2

Trawl Gear Interference with Pipelines

This chapter contains a brief description of typical bottom trawl gear used in Norwegian Waters. Interference from these types of gear is further categorized in order to illustrate different load effects and pipeline response during interference. In addition, the DNV-RP-F111 calculation method for estimating clump weight pull-over design loads and the experimental tests which forms the basis of this method is described.

2.1 Trawl Gear

Trawling nowadays is carried out by a range of ship sizes and type of gear. Trawling may be performed by one vessel or pair trawling using two vessels. The trawling velocity and type of gear are mainly governed by the movement pattern and swimming speed of target species. Trawling for prawns is typically performed at 1-1.5 m/s, whereas for fish up to 2.8 m/s [3]. The trawl gear differ mainly in terms of how the trawl net is kept open and whereas the trawling is performed at the seabed bottom or midwater. In Norwegian waters, bottom trawling with one vessel is the most used trawling configuration [10]. Bottom trawl gear operated by a single vessel can further be divided into two main categories, beam trawls and bottom otter trawls.

2.1.1 Beam Trawl

Beam trawls derive their name from the transverse beam that keeps the trawl net open. Beam trawls are normally operated in pairs towed by outriggers on each side of the vessel. Beam shoes are fitted in order to slide across the seabed and prevent sinking into soft ground. An advantage with the beam trawls is that the trawl net is kept open regardless of trawling speed. However, the spreading height of the trawl net is very limited, up to 1 m, making beam trawls unsuited for most target species in Norwegian waters [9]. However, the Dutch fishing industry operates beam trawls successfully fishing for high priced flatfish in the southern parts of the North Sea [10]. An illustration of a typical beam trawl and trawling configuration is given in figure 2.1.

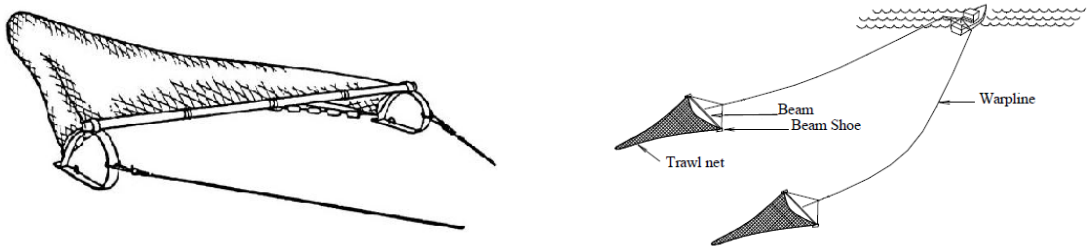

(a) Beam trawl [5]

(b) Pair beam trawl configuration [3]

Figure 2.1: Beam trawl gear

2.1.2 Otter Trawl

The otter trawl is the most common bottom trawl gear used in Norwegian Waters [10]. The typical otter trawl consists of a single trawl net which is kept open by the hydrodynamic spreading force from two trawl doors, one at each side. The trawl doors are attached to the trawl net by sweep lines and to the vessel by two warp lines, as illustrated in figure 2.2. In order to obtain a constant and sufficient spreading of the trawl net, the spreading force have to overcome both the tension forces in the warp line and sweep line. This limits how low velocity the trawl gear can be operated in. In addition, the trawl doors must be heavy in order to prevent the upward pull from the warp lines in lifting the trawl nets from the seabed. The largest trawl doors can be up to 6 tons and are used in the Barents Sea [3].

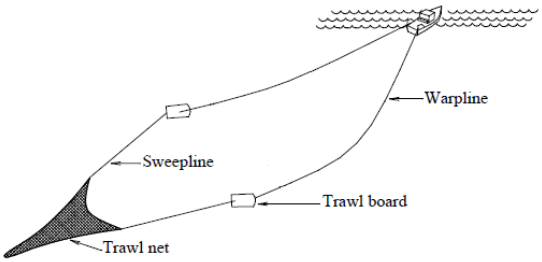

Figure 2.2: Otter trawl [3]

2.1.3 Twin Trawl and Applications of Clump Weights

A recent development of the otter trawl is the twin trawl, where two trawl nets are towed side by side from a single vessel. Using two trawl nets increases the catch rate and efficiency of the trawler. Thus, governed by catch and cost optimization the use of twin trawl systems is expected to become more popular in the future [7].

A typical twin trawl configuration is illustrated in figure 2.3. Compared to a conventional otter trawl, the twin trawl consists of an additional center warp line and a clump weight in the middle. One advantage with this is that most of the towing resistance is transferred through the center warp line and thereby lowering the tension in the outer warp lines. This reduces the necessary spreading force from the trawl doors and results in a larger opening of the trawl nets. However, as most of the towing resistance is transferred through the center warp line, the upward pull from the warp line increases and clump weights are presently of the heaviest trawling equipment in use.

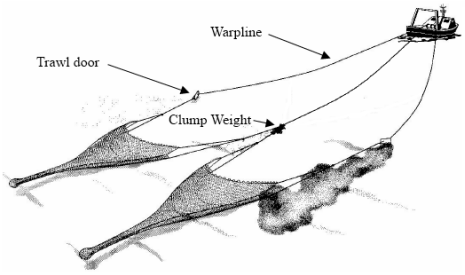

Figure 2.3: Twin trawl [7]

Several clump weight designs are used, ranging from just clumps of chains, to special purpose built bobbin and roller types. A bobbin type is illustrated in figure 2.4a and a roller type in figure 2.4b. Clumps of chains are typically used by smaller vessels and weighing less than 2 tons, bobbin types are typically 2 to 3.5 tons, whereas roller types are the ones being used on larger trawlers and are typically 3.5 to 9 tons, numbers from [7]. A clump weight mass of 5 to 6 ton is typical trawling for fish in the North Sea and Norwegian Sea, whereas the largest clump weights can be up to 10 tons and are used in the Barents Sea and outside Greenland mainly trawling for prawns [7].

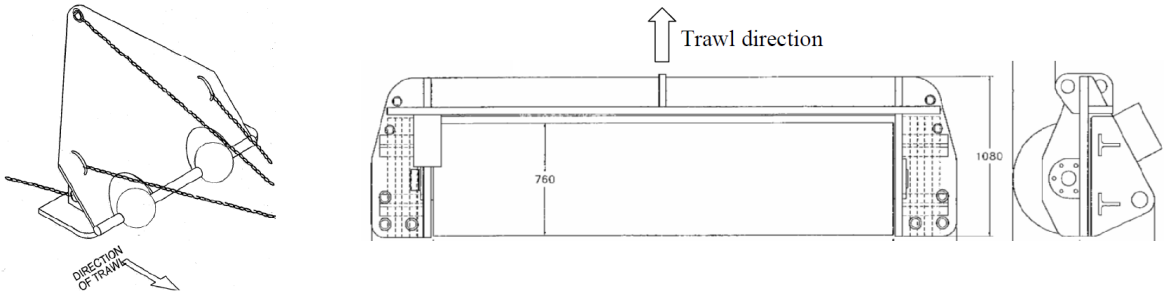

(a) Bobbin type

(b) Roller type

Figure 2.4: Illustration of special purpose built clump weight designs [3]

2.2 Trawl Gear and Pipeline Interaction

When bottom trawl gear is towed across a pipeline, the collision may be divided into two stages; the initial impact and subsequent pull-over phase, which of defines two different load effects from trawl gear interference.

The initial impact will typically last for some hundreds of a second, where the trawl gear is stopped and the kinetic energy or impact energy of the trawl gear is transferred to the pipeline. This may cause local damage to the pipeline coating and steel wall. The loads imposed to the pipeline in this case is mainly governed by the mass, velocity and front shape of the trawl gear, see figure 2.5a.

The subsequent pull-over phase last from some 1-10s, resulting in a more global deformation of the pipeline as the trawl gear is gradually rotated over the pipeline. The loads imposed to the pipeline during this stage is mainly governed by the required warp line tension necessary to free the trawl gear from the pipeline. Especially for clump weights, the magnitude of pull-over loading may be substantial considering the large mass and position during pull-over, as illustrated in figure 2.5b. This position is from now on referred to as "a temporary hooking effect" of the clump weight and must not be interpreted as "hooking".

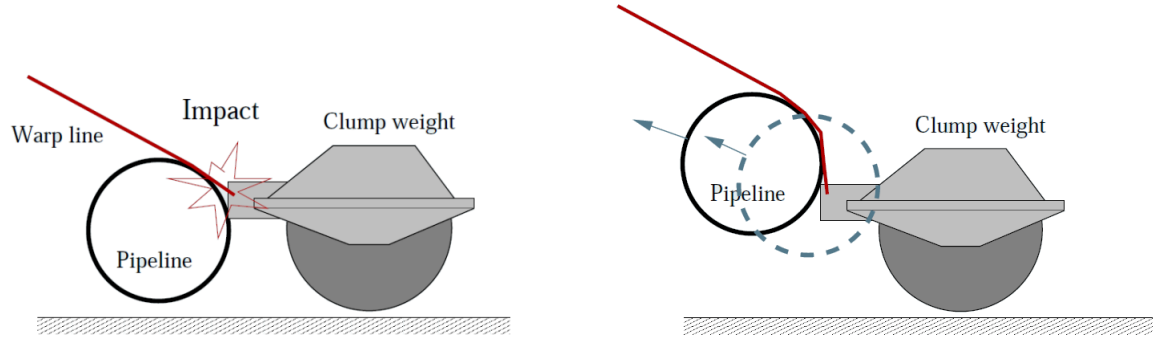

(a) Initial impact

(b) Pull-over

Figure 2.5: Clump weight interaction stages [1]

Hooking is a special case of trawl gear interference when the trawl gear is stuck under the pipeline forcing the trawler to stop, back up and try to free the trawl gear, see figure 2.6. In this case, forces as large as the breaking strength of the warp line may be applied to the pipeline. However, hooking of trawl gear is an rare event, only 7 events of hooking were reported on the Norwegian Shelf between 2000 and 2003.

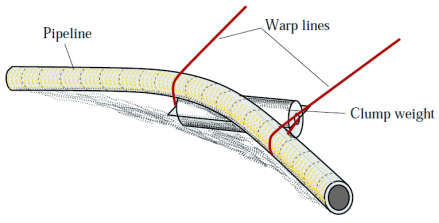

Figure 2.6: Hooking of trawl gear [1]

2.3 DNV-RP-F111

In engineering, trawl gear design loads are generally implemented according to DNV-RP-F111 - *Interference Between Trawl Gear and Pipelines*. This recommended practice was published in 2005 and aims specifically to provide guidance on applicable design methods and rational design criteria regarding trawl gear interference in pipeline design.

Calculation methods for three aspects of trawl gear interference are covered, the initial impact, pull-over and hooking of trawl gear. The design methods are based on collected data of typical trawl gear used in the North Sea and Norwegian Sea up to 2005 including, interference from beam trawl, trawl doors and clump weights.

The following sections will describe the calculation method provided to estimate pull-over design loads for clump weights. This calculation method is based on experimental tests. Hence, the validity range of this design method reflects the test configuration, i.e. only valid for rigid pipelines between 10" - 40" in diameter and for bobbin or roller type clump weights. A more detailed description of these tests will be given in Section 2.4.

2.3.1 DNV Pull-over Response Calculation

According to DNV, it is recommended that a dynamic analysis is carried out to calculate the pull-over response from trawl gear. A static analysis, neglecting pipeline inertia forces is most likely to be non-conservative in terms of localization of bending. The modeled length of the pipeline must be sufficient to represent pipeline to soil interaction and avoid influence from boundary conditions. All relevant non-linear effects shall be included, such as but not restricted to;

- buckling effects caused by effective axial force,
- large displacements including geometrical stiffness,
- soil resistance,
- non-linear material behavior.

The pull-over load is to be applied as a single point load represented by a force time history.

2.3.2 Maximum Pull-over Force for Clump Weights

The magnitude of the pull-over load is calculated according to the pipeline and clump weight properties as illustrated in figure 2.7. Further, the pull-over load is divided into a horizontal and vertical contribution. The maximum horizontal pull-over force is calculated according to equation 2.1,

$$F_p = 3.9 \cdot m_t \cdot g \cdot \left(1 - e^{-1.8 \cdot h^{'}}\right) \cdot \left(\frac{OD}{L_{clump}}\right)^{-0.65} \tag{2.1}$$

$$h^{'} = \left(H_{sp} + OD\right)/L_{clump} \tag{2.2}$$

where OD is the outer diameter of the pipeline, including coating. L_{clump} is the distance from the clump weight center of gravity to point of reaction, H_{sp} is the span height measured from the seabed gap and m_t is the clump weight steel mass.

The maximum horizontal pull-over force versus span height for the clump weight configuration applied in the simulations are illustrated in figure 2.8, and shows how the horizontal pull-over force converges to an asymptotic value as the span height increases.

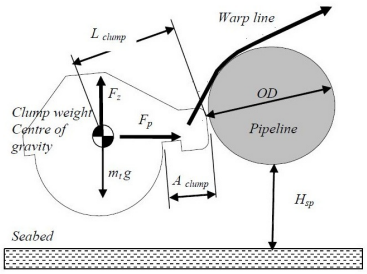

Figure 2.7: Clump weight interaction [3]

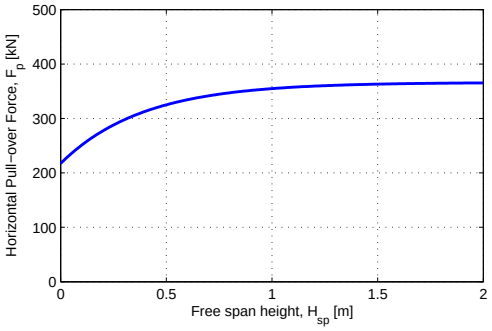

Figure 2.8: Maximum horizontal pull-over force vs span height

The maximum vertical pull-over forces are dependent on F_p, and both upward and downward force are to be considered in determining the most critical load combination. The maximum upward vertical force can be calculated according to equation 2.3 and maximum downward force according to equation 2.4.

$$F_z = 0.3Fp - 0.4 \cdot m_t \cdot g \tag{2.3}$$

$$F_z = 0.1Fp - 1.1 \cdot m_t \cdot g \tag{2.4}$$

2.3.3 Pull-over Force-time History for Clump Weights

The applied pull-over force-time history for clump-weights are given in figure 2.9. The force-time history can be understood as the first 0.2s is the initial impact were the clump weight is stopped. From that point the load increases linearly while the warp line is tensioned and the clump weight is gradually rotated over the pipeline, assuming a temporary hooking effect of the clump weight. The clump weight is released at maximum force.

The duration of the force-time history can initially be estimated according to equation 2.5,

$$T_p = Fp/\left(k_w \cdot V\right) + \delta_p/V \tag{2.5}$$

where k_w is the warp line stiffness, V is the trawling velocity and δ_p is the global pipeline displacement at the point of interaction. The pipeline displacement is however not known prior to the response analysis and must therefore be assumed and corrected in an iterative procedure to determine the pull-over duration.

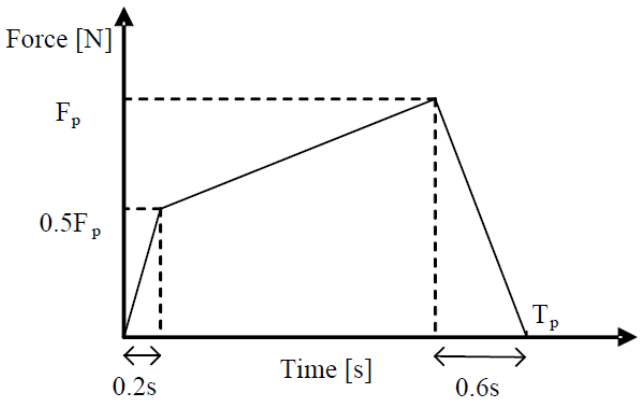

Figure 2.9: Force-time history for clump weight pull-over force on pipeline [3]. Applies for both lateral and vertical pull-over forces,F_p and F_z.

2.4 Clump Weight Pull-over Tests

In connection with the Kristin and Snøhvit field developments in the Norwegian Sea, Statoil carried out a model test to investigate pull-over forces from clump weights on free spanning pipelines. A total of 139 tests were performed at MARINTEK's Ocean Laboratory in June/July 2004. The result from these tests forms the basis for the calculation method provided in DNV-RP-F111. The model test results have been made available to the thesis for verification purposes, thus a brief description of the model test will be given in this section [16].

2.4.1 Model Scale

The model scale was 1:10 according to the principles of Froude's law. The test results were corrected for a water density 1025 kg/m^3 and all data presented as full scale measurements. Hence, all dimensions specified in this section and further on are given as full scale values.

2.4.2 Free Spanning Pipelines

Three different pipe diameters were tested, 350 mm, 530 mm and 840 mm. The pipes were ballasted by a combination of divinycell (foam), water and lead to achieve the target mass. The length of the modeled pipeline was 25m. The span height was varied over six different heights, 0.0 m, 0.25 m, 0.50 m, 0.75 m, 1.0m and 4.0 m. The pipe end condition was fixed, flexible or trenched.

For the flexible conditions, linear springs and dampers were applied to the pipe ends to represent the overall pipeline stiffness.

2.4.3 Twin Trawl Gear

A complete twin trawl rigging was supplied by SINTEF Fisheries and Aquaculture, Hirtshals, Denmark, including trawl nets, sweep lines, warp lines, trawl doors and clump weight. The trawl nets and sweep lines where included to give a correct representation of trawl net drag resistance and tension to the sweep lines and warp lines. The outer warp lines where attached to the trawl doors, the center warp line to the clump weight. The upper ends of the warp lines were fixed to a towing carriage. The water depth was 350 m and the warp line length was 895m including springs to represent two different warp line stiffness's of 30 kN/M and 60 kN/M. The warp line length was chosen to facilitate a warp angle of 23°.

Each trawl door had a dry weight of 3.8 tonnes and was a model scale version of the Thyborøn 135" trawl door. The tests were performed with two different types of clump weights, a roller and bobbin type, as given below and illustrated in figure 2.10

- Thyborøn roller type steel model - Ballasted to 6.1 tonnes dry weight
- Poly Ice bobbin type steel model - Ballasted to 3.6 tonnes dry weight

(a) Bobbin type (b) Roller type

Figure 2.10: Illustration of clump weights used in the experimental tests [16]

2.4.4 Test Procedure

The test procedure for each test may in general be described as following:

- The twin trawl was laid out on the bottom, at start position.
- The test rig made ready with the correct parameter settings.
- Start of towing carriage.
- The towing carriage was towed at a constant velocity.
- Stabilization of the trawl gear into normal spreading and towing position.
- Interaction between center warp line, clump weight and pipeline recorded. The trawl doors went outside the test rig.
- Retardation of the tow, the trawl nets did not interact with the test rig.

2.4.5 Data Acquisition and Test Results

Horizontal and vertical pull-over force, warp line force and pipeline horizontal displacement were measured during interaction.

Force transducers at each end of the test pipe was installed to measure the interaction forces parallel and normal to the towing direction, which of the sum of these forces was taken as the horizontal and vertical pull-over force, respectively. The pipeline displacements were measured at each end and the mean position taken as the horizontal pipeline displacements during interaction.

The obtained test data was transformed into and presented as time histories. All of the force and position histories were low pass filtered to remove signal vibrations from the result.

In general, the following could be seen from the test results:

- The horizontal pull-over force seemed to increase with increasing span height for all pipe diameters.
- The horizontal pull-over force decreased for increased pipe diameter.
- The horizontal pull-over force was larger for the 6.1 ton Thyborøn roller type than for the 3.6 ton Poly Ice bobbin type.
- The warp line forces during pull-over seemed to follow the same tendency as the horizontal pull-over force, as stated in the tree points above.
- The vertical pull-over forces were an order of magnitude smaller than the horizontal pull-over forces.

To examples of measured horizontal pull-over force for different warp line stiffness and clump weight mass is given below.

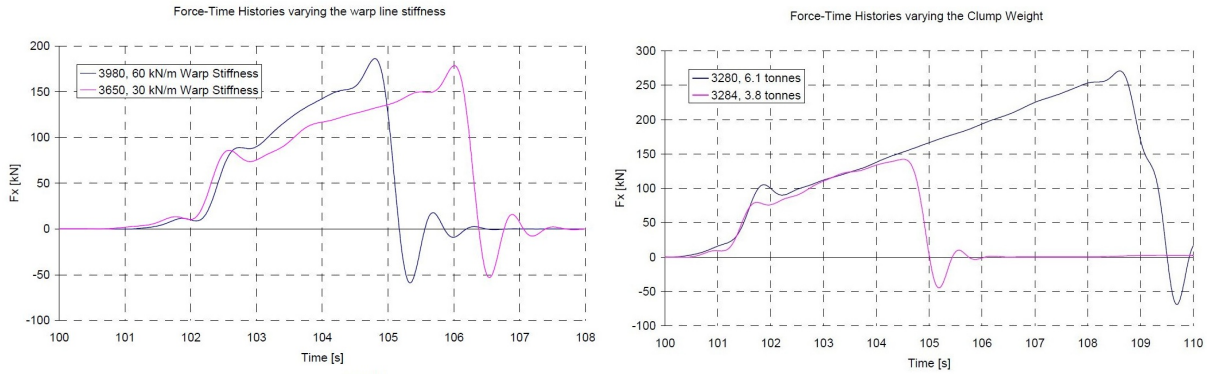

(a) Different warp line stiffness

(b) Different clump weight mass

Figure 2.11: Force-time histories from experimental tests [7]

Chapter 3

Finite Element Analysis

The software SIMLA has been used throughout all simulations in this thesis work. SIMLA is developed by MARINTEK and is a special purpose FEM based program system for non-linear static and dynamic analysis of pipelines. This includes a fairly general set of powerful contact elements applicable for a range of interaction problems.

A dynamic finite element analysis was applied in all simulations to include inertia forces during interference. The solution methods applied in SIMLA are not discussed any further, reference is made to the SIMLA Theory Manual [17] and existing literature on the subject [2] and [15]. However, a brief introduction to non-linear effects and application in SIMLA are given the following sections.

3.1 Non-linear Effects

In structural analysis, non-linear effects can in general be classified into three different categories [2].

- **Material non-linearity**, which in brief may be associated to a non-linear stress-strain relationship as the stresses level exceeds the material yield limit.

- **Geometrical non-linearity**, arises when the deformations are large enough such as the equilibrium equations must be expresses according to the deformed shape of the structure.

- **Contact non-linearity**, arises when different structures, or different surfaces of a single structure either come in contact, separate or slides on one another with friction. Contact forces are either gained or lost and must be determined in order to calculate structural behavior.

The problems stated above become non-linear due to the stiffness and loads become a function of displacements or deformations and in general an incremental and iterative procedure is required to solve for the displacements and stiffness relationship.

3.2 Application of SIMLA

Simulation of clump weight interference may be regarded as a highly non-linear problem. Contact problems in general are non-linear and often highly so due to large and sudden stiffness changes as contact is made [2]. Due to the magnitude and duration of the pull-over load, large pipeline deflections and displacements may be expected during interference, which further may induce yielding of the material. In addition, the pipeline will interact with the seabed continuously during interference, either penetrating, lifting or sliding along the seabed requiring a sufficient representation of soil resistance and interaction. All of witch may be regraded as non-linear effects.

The degree of non-linearity present in the system may to a large extent increase the analysis complexity and computational costs in order to solve the problem. SIMLA is equipped with efficient solution and modeling techniques in order to include and solve for all of the problems stated above. The following chapter will describe how these effects are included in the SIMLA model.

Chapter 4

SIMLA Modeling

This chapter will describe all aspects of modeling in order to simulate clump weight pull-over interference, including definition of input parameters, seabed interaction and special considerations made in modeling of the clump weight and pipeline interaction. Further, the method used to extract pull-over forces from SIMLA and a description of the general simulation procedure is presented at the end of this chapter.

4.1 Trawl Gear Configuration

The same trawl gear configuration have been used in all simulations and is consistent with the twin trawl rigging used in the experimental tests, including a roller type clump weight, trawl nets, center warp line and sweep lines, as illustrated in figure 4.1 and 4.2.

The trawl nets are represented by two drag nodes and a specified drag coefficient at the end of each sweep line. The applied drag coefficient have been calibrated according to the experimental test results, such as the tension in the warp line during constant towing velocity corresponds to the measured warp line tension in the experimental test. Further, the trawl nets are modeled without mass properties in order to avoid compression forces in the sweep lines during interference. The sweep angle was assumed equal to 20 °in all simulations and given a vertical angle, ψ, to represent 18" steel bobbins between the trawl nets and sweep lines. The warp line angle is 23°and the warp line surface node, or towing node is gradually accelerated to 1.95 m/s by applying prescribed displacements. The trawl gear data is given in table 4.1.

Quantity	**Symbol**	**Value**	**Unit**
Depth	d	350	m
Trawling velocity	V	1.95	m/s
Warp angle	ϕ	23	deg
Sweep angle	θ	20	deg
Vertical sweep angle	ψ	0.3	deg
Trawl net drag coefficient	C_d	20.8	m^2
Trawl net mass	m	0.0	kg

Table 4.1: Trawl gear data

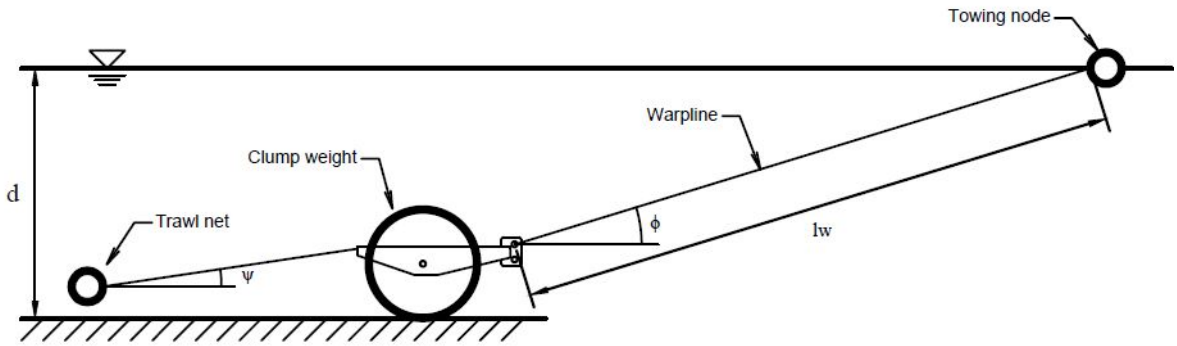

Figure 4.1: Trawl gear configuration, vertical plane

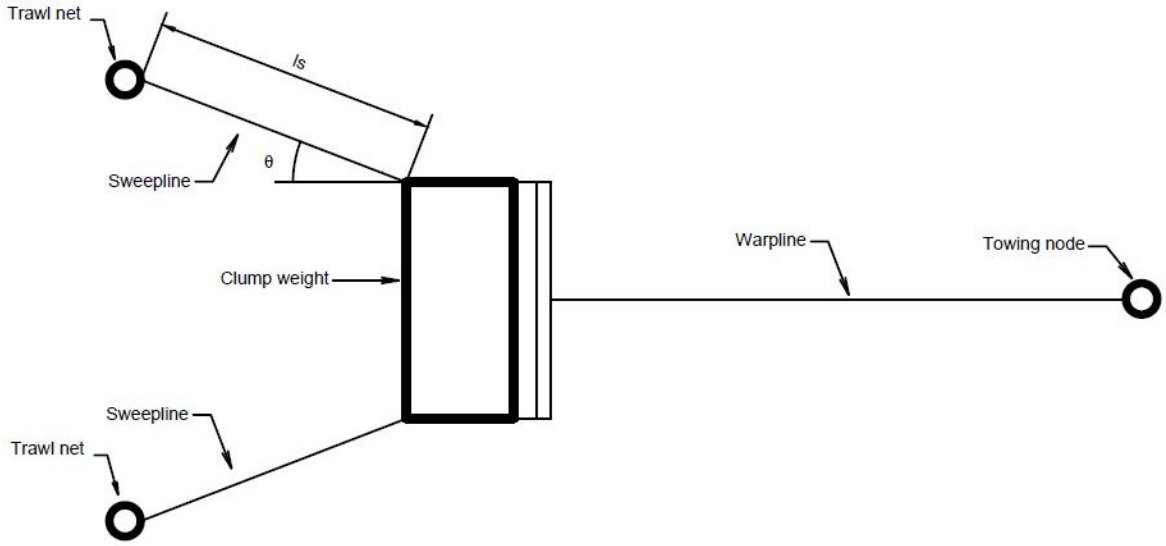

Figure 4.2: Trawl gear configuration, horizontal plane

4.1.1 Warp Line

The warp line is modeled in two parts. The upper part of the warp line is modeled with one single cable element without mass and drag properties and will function as a linear spring. The axial stiffness of the warp line is according to the experimental tests 30 kN/m. The lower part of the warp line, which may be in contact with the pipeline, is 1.8m in length and modeled by 130 linear pipe elements. A denser mesh was applied close to the clump weight attachment point to achieve a consistent contact interface. The bending stiffness of the lower part was set as low as possible to allow bending of the warp line during interaction.

Linear pipe elements have to be assigned a certain mass. Due to the short length of the lower part of the warp line, unnatural oscillations occurred when the warp line was coupled to the sea environment. To avoid this, the lower part of warp line was modeled without sea contact i.e. no added mass or drag forces was included and submerged weight of the lower part will be equal to weight in air. However, in verification of the contact model a good agreement with experimental tests was achieved with the simplified warp line properties indicating that warp line excitations are not decisive for the pull-over result.

Quantity	Symbol	Value	Unit
Length	l_{lw}	1.80	m
Axial stiffness	EA	26.8	MN
Bending stiffness	EI	1.50	kNm^2
Added mass coefficient	C_a	0.0	-
Drag coefficient	C_d	0.0	-
Structural mass	m	4.0	kg/m
Submerged weight	w_s	4.0	kg/m

Table 4.2: Lower warp line properties

Quantity	Symbol	Value	Unit
Length	l_{uw}	893.2	m
Axial stiffness	EA	26.8	MN
Added mass coefficient	C_a	0.0	-
Drag coefficient	C_d	0.0	-
Structural mass	m	0.0	kg/m
Submerged weight	w_s	0.0	kg/m

Table 4.3: Upper warp line properties

4.1.2 Sweep Lines

The sweep lines are 40 m in length according to the experimental tests and modeled with single cable elements. Convergence of the analysis was found sensitive to the axial stiffness of the sweep lines and the sudden acceleration experienced when the clump weight is released from the pipeline. Increasing the axial stiffness of the sweep lines allow the analysis to continue after onset of maximum pull-over force. Hence, an axial stiffness of 40 MN/m was applied for the sweep lines. The obtained pull-over force was shown to be insensitive to the axial stiffness of the sweep lines.

Quantity	Symbol	Value	Unit
Length	l_s	40.0	m
Axial stiffness	EA	40	MN
Added mass coefficient	C_a	1.0	-
Drag coefficient	C_d	1.0	-
Structural mass	m	0.0	kg/m
Submerged weight	w_s	0.0	N/m

Table 4.4: Sweep line properties

4.1.3 Clump Weight

The clump weight model is based on the Thyborøn roller type clump weight used in the experimental tests. Only perpendicular crossing at midspan of the pipeline was simulated, thus the clump weight was kept from lateral translation and was only allowed to rotate about the longitudinal axis of the clump weight, i.e. the clump weight will hit level and parallel to the pipeline at midspan.

Specific dimensions and mass distribution was however not initially clear from the MARINTEK report, [16]. Further research was necessary in order to model the clump weight correctly. According to records, measurements of a similar scale model were obtained from SINTEF Fisheries and Aquaculture, Hirtshals, Denmark. According to SINTEF the clump weight had a total dry mass of 3840 kg and the roller length was 1.55 m. SINTEF also stated that no additional ballast weights where delivered. The clump weight model reflects the specification provided by SINTEF, assuming that the additional ballasting to 6100 kg was performed at site and placed inside the hollow roller. The measurements and an illustration of this clump weight are given in Appendix B. The cross section properties were taken from drawings provided from manufacturer, Thyborøn Skipsmedie AS, Denmark, which are attached in Appendix A.

The model includes a simplified geometry of the clump weight roller, frame and warp line bracket. The entire clump weight was modeled with rigid linear pipe elements, assuming that the clump weight will not deform and dissipate energy during impact. The roller is 1.55m in length and modeled with two pipe elements with a diameter 0.76m. In addition 130 circumferential contact elements were used to define the outer geometry of the clump weight roller. The contact interaction between the clump weight and pipeline will be further described in Section 4.4. The clump weight roller was coupled to the frame by applying constraints in translational degrees of freedom allowing the clump weight roller to rotate during towing. As only the lower part of the frame will be in contact with the pipeline and pull-over forces is transferred only to the mid node of the pipeline, vertical and lateral extension of the frame was neglected. The warp line bracket is modeled with one single pipe element of which the extension is equal to the straight front edge of the warp line bracket. The clump weight model and drawings are illustrated in figure 4.3 and 4.4.

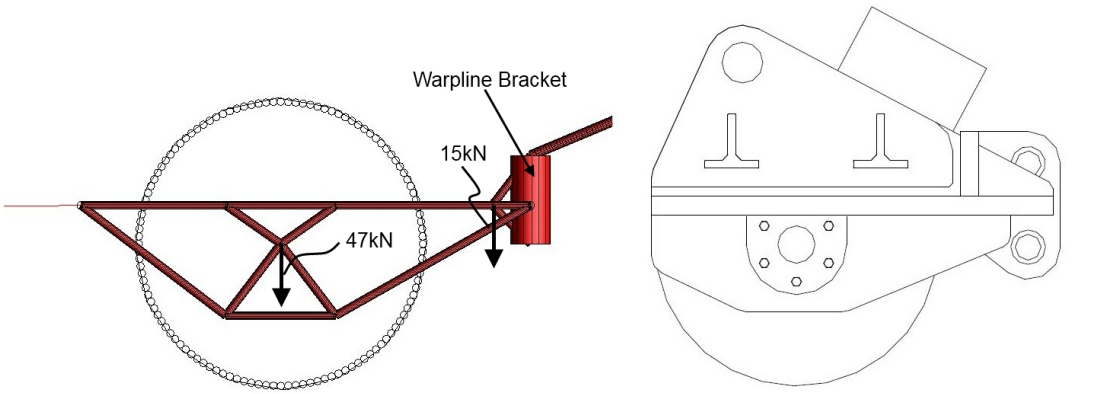

(a) Clump weight model

(b) Thyborøn roller type, cross-section drawing

Figure 4.3: Clump weight cross-section properties

As illustrated in figure 4.3a, the clump weight was modeled including an extension of rear part of the frame which corresponds to the sweep line attachment points of model scale clump weight illustrated in Appendix B. This extension is however of less significance for the pull-over response.

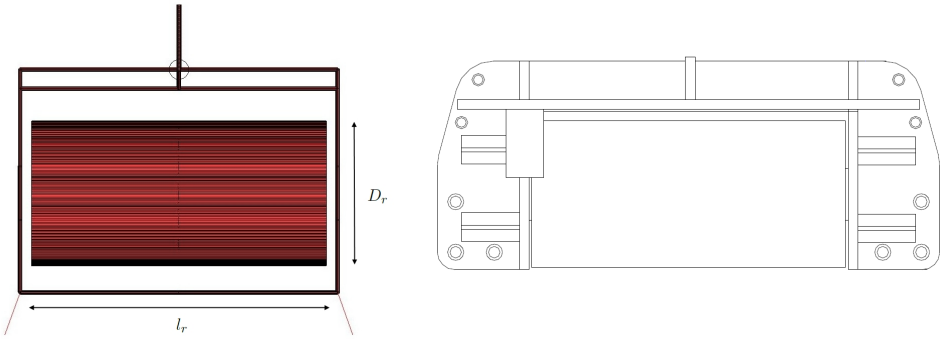

(a) Clump weight model (b) Thyborøn roller type, cross-section drawing

Figure 4.4: Clump weight, horizontal plane

The mass distribution of the clump weight was found to influence the magnitude of the pull-over load. For that reason the mass of the front part of the frame was applied separately along a second front beam, as illustrated in figure 4.3a . The remaining mass was assumed to act along the center line of the of the clump weight roller.

Added mass of the clump weight was calculated according to DNV-RP-F111 considering a 0.76 m in diameter cylinder, with length equal to 1.55 m. An added mass coefficient of 2.29 was used to account for seabed proximity and an reduction factor of 0.8 applied to account for cylinder length [4]. Contribution from entrained water in the hollow roller was neglected due to uncertainties in how the clump weight was ballasted. It is assumed that the additional ballast is placed inside the hollow roller and no water is entrapped.

Quantity	**Symbol**	**Value**	**Unit**
Roller diameter	D_r	0.76	m
Roller length	l_r	1.55	m
Dry weight	m_t	6100	kg
Added mass	m_a	1320	kg
Submerged weight	w_s	52	kN

Table 4.5: Clump weight properties

4.2 Pipeline Models

Three different SIMLA models have been established to simulate clump weight pull-over interference:

1. A contact model to simulate the experimental tests. This model was initially created for verification purposes and is referred to as “The Experimental Test Model”.
2. A contact model to simulate clump weight interference with a free spanning pipeline, referred to as “The Free Spanning Pipeline Model”.
3. A point load model to calculate DNV-RP-F111 pull-over loads.

The point load model is identical to the free spanning pipeline model apart from the clump weight interaction is represented with a point load, hence only the contact models are described in this section. The trawl gear configuration and contact interfaces are identical for both contact models.

4.2.1 Experimental test model

The experimental test model corresponds to a full scale model of the test configuration described in Section 2.4. Hence, all values presented in this section are given in full scale and not model scale dimensions. The experimental tests were performed with only a small section of the pipeline and for three different pipeline diameters. In this case only the 350 mm pipeline diameter configuration has been modeled.

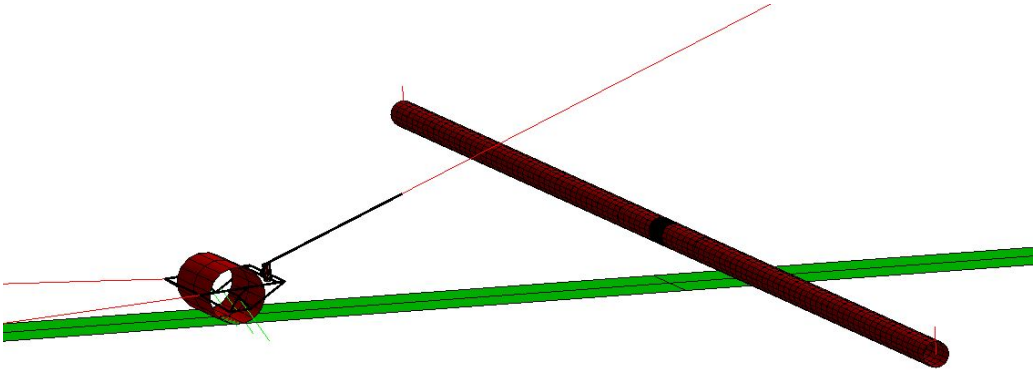

Figure 4.5: Illustration of the experimental test model

The pipeline section is 25 m in length and made almost totally rigid to account for scaling effects. Due to the short length of the model an element size of 0.25 m was used for the entire pipe length. For the simulations with fixed end condition, the pipeline was restrained against translation and rotation at both ends. Flexible end conditions are modeled using springs at both ends allowing the pipeline to move in lateral direction. From analysis it became evident that some pretension of the springs was necessary to obtain pipeline displacements of correct order. It was later confirmed by the author of the MARINTEK report [16] that some pretensioning also was present during the testing. With a pretensioning of 80 kN a good agreement regarding pipeline displacements was achieved. The pretensioning was included in the material curve defining the spring stiffness as illustrated in 4.6. Damping was also introduced in each spring element.

Quantity	**Symbol**	**Value**	**Unit**
Length	L	25	m
Pipe diameter	OD	350	mm
Structural mass	m	405.9	kg/m
Submerged weight	w_s	307.3	kg/m
Added mass coefficient	C_a	1.0	-
Drag coefficient	C_d	1.0	-
Pipe end pretensioning	F_s	80	kN
Pipe end stiffness	k_s	40	kN/m
Pipe end damping	c_s	5	kN/m/s

Table 4.6: Test pipe properties

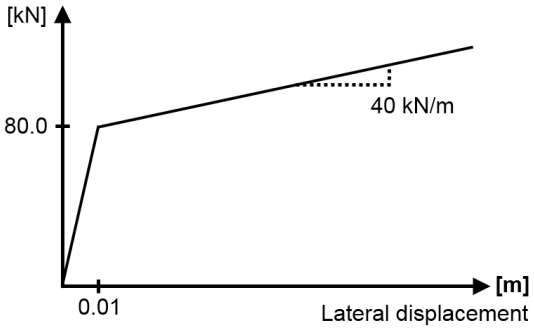

Figure 4.6: Spring stiffness material curve

4.2.2 Free Spanning Pipeline Model

The free spanning pipeline model was created to investigate pull-over forces on a flexible pipeline configuration, including, in addition to realistic soil properties, both lateral and vertical flexibility. The length of the model is 1000 m and includes a 50 m free span. The pipeline is fixed at each end assuming rock dumping has been used to anchor the pipeline. As for the experimental test model, in order to use the same set of contact elements, the pipeline outer steel diameter is 350 mm. The wall thickness was chosen to 20 mm and the modeled pipeline reflects a typical small diameter pipeline.

The entire pipeline length was modeled with 270 linear pipe elements. An element size of 14.0 m was used at the outer edges of the model, which are not displaced during interference. The element size is gradually reduced to 0.20 m at point of interference. The pipeline is modeled with linear material properties and is assumed without coating and in empty condition, i.e. no content, internal pressure or temperature loading was included. These assumption and simplifications were taken to reduce modeling efforts and computational time in order to provoke a general flexible pipeline response during pull-over. The pipeline mass and stiffness properties reflect the steel pipe cross-section. Span height was varied by adjusting the pipeline and seabed depth. The trawl gear configuration was kept at a constant depth in all simulations.

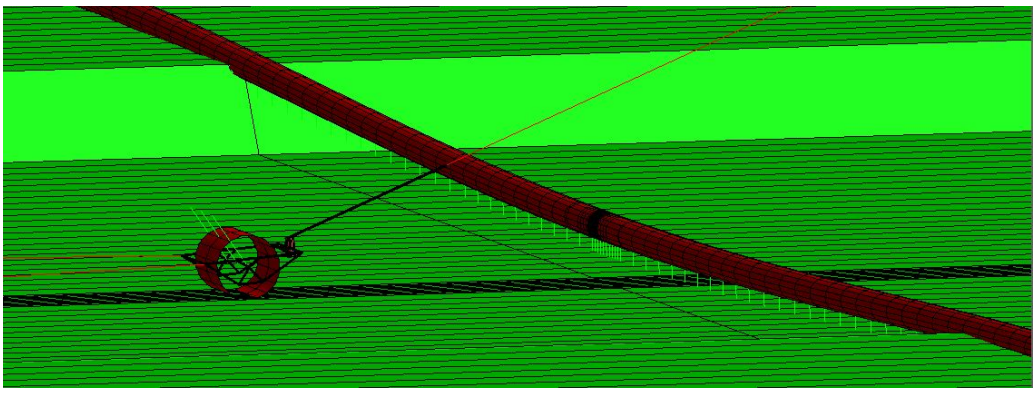

Figure 4.7: Illustration of the free spanning pipeline model

Quantity	Symbol	Value	Unit
Length of pipeline model	L	1000	m
Free span length	l_{fs}	50	m
Pipe diameter	OD	350	mm
Pipe wall thickness	t_w	20	mm
Structural mass	m	162.7	kg/m
Submerged weight	w_s	64.2	kg/m
Added mass coefficient at free span	C_a	1.0	-
Added mass coefficient at seabed	C_a	2.29	-
Drag coefficient	C_d	1.0	-
Axial stiffness	EA	4350	MN
Bending stiffness	EI	59.5	MNm^2
Elastic modulus	E	210	GPa

Table 4.7: Pipeline properties

4.3 Seabed Interaction

In this section the clump weight and pipeline seabed interaction is described. The seabed is modeled completely flat along the entire length of the pipeline and path of the clump weight. In the experimental test model only a small strip of the seabed, which the clump weight is towed along, is included. Hence, the pipeline to seabed interaction presented in this reflects the free spanning pipeline model. The small strip defining clump weight to seabed interaction is identical in both contact models.

In SIMLA, seabed interaction is modeled using special purpose seabed contact elements. A contact surface representing the seabed is created between lines or routes along the seabed. Different soil properties can be assigned to each line which is kept until next line defines a new set of soil properties. Interaction is represented by applying springs at each node for the pipe segment in contact. Friction can be applied in axial and lateral direction, with interaction curves defining the unit friction force per meter displacement. SIMLA applies a scaling factor to these interaction curves and Coulomb friction is applied per unit length in contact with the seabed. In vertical direction a force-displacement curve per unit length in contact is used to represent vertical soil resistance. The scaling factor applied to the interaction curves presented in this section has been set equal to 1.0 in all cases.

4.3.1 Pipeline

In the free spanning pipeline model, seabed contact elements are included at all pipeline nodes. The free span is introduced by lowering the seabed between one element length at each side. Friction is applied in axial and lateral direction as illustrated by the interaction curves in figure 4.8 and 4.10. In lateral direction an additional interaction curve is used to define pipeline breakout resistance, illustrated in figure 4.9. The additional interaction curve is set to be active for penetrations larger than 0.07m. The applied resistance coefficients was supplied by Reinertsen AS and are estimates for a 12" pipeline in soft clay. The vertical soil resistance is represented by a constant sloping force displacement curve as illustrated in figure 4.11 and has been chosen to allow the pipeline to penetrate the seabed 1/5 of the outer diameter at the free span shoulders.

4.3.2 Clump Weight

The clump weight to seabed interaction is defined at three nodes along the clump weight roller. The small strip of the seabed which the clump weight is towed along is assigned individual soil properties and is as wide as the clump weight and stretches across the model in towing direction. In lateral direction of the clump weight roller the friction coefficient was set to equal 1.0 to make the clump weight roll and not slide along the seabed floor. In axial direction the clump weight is restrained from translations. A high vertical soil resistance was applied to prevent the clump weight from sinking down into the seabed. The applied lateral and vertical interaction curves are illustrated in 4.8 and 4.11.

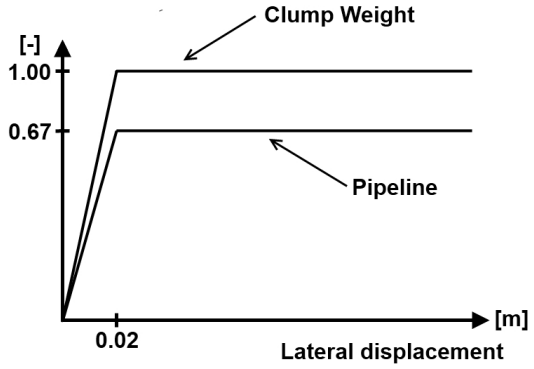

Figure 4.8: Lateral seabed interaction curve

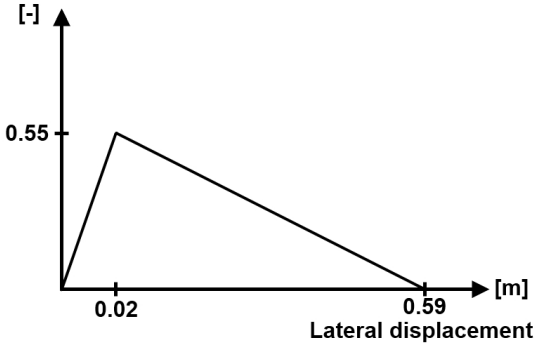

Figure 4.9: Additional seabed interaction curve

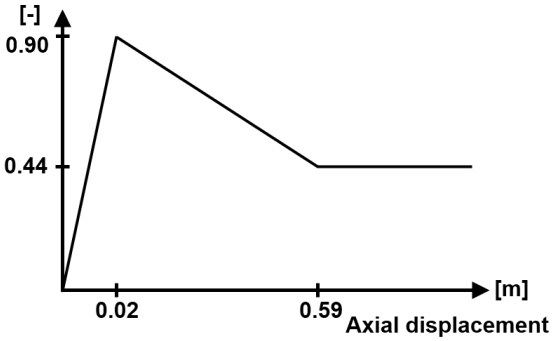

Figure 4.10: Axial seabed interaction curve

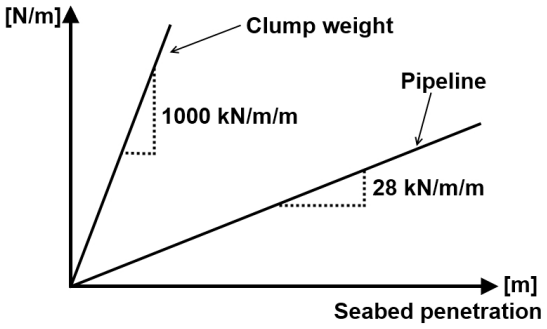

Figure 4.11: Vertical seabed interaction curve

4.4 Clump Weight and Pipeline Interaction

The clump weight to pipeline interaction is modeled by defining groups of slave elements and corresponding groups of master elements. The slave element groups contain a set of structural pipe elements, whereas the master element group contains a set of contact elements. In SIMLA, different types of contact elements are available for different purposes. In this case cont164 roller elements, from now on referred to as master rollers, were used for all contact interfaces.

The main purpose of the master rollers is to determine and establish contact with the slave elements during interaction. The master rollers search for the position of the slave elements at every time increment. If the slave element is inside the master roller search area, the distance or gap between the outer shell of the slave element and the master roller is calculated. If the gap is negative, i.e. the slave element has penetrated the master roller, contact is establish and contact forces are transferred [17].

The clump weight to pipeline interaction was modeled with four contact interfaces defining the geometry in contact with the pipeline, as given below and illustrated in figure 4.12. To obtain a consistent contact interaction during pull-over, special consideration has been made upon the arrangement of both slave elements and master rollers. This is further described in section 4.4.2.

Only the warp line and warp line bracket interaction was found necessary to simulate the pull-over interference for span heights above 0.25 m, as the clump weight was stopped and rotated about this point. However applying a complete set of contact interfaces may be necessary to account for special cases of clump weight behavior or lower span heights, where rotation about the warp line bracket does not govern the clump weight response. This was the case for simulating a lower warp line attachment point. Illustration 4.12b and 4.12c is from this simulation.

Warp Line

The warp line interaction is illustrated in figure 4.12a and was modeled with one single master roller. The master roller is coupled to the mid-node of the pipeline and of same diameter as the pipeline, 350mm. The lower part of the warp line consists of 130 linear pipe elements arranged in a single slave element group. A denser mesh was applied close to the warp line bracket to account for warp line bending and avoid loss of contact when the warp line slides relative to the pipeline.

Clump Weight Frame

The clump weight frame interaction was modeled in same way as the warp line interaction with one large master roller connected to the mid-node, as illustrated in 4.12b. Only the sloping front part of the frame was included in a corresponding slave group.

Clump Weight Roller

The clump weight roller interaction was modeled with 120 circumferential master rollers on the clump weight and rigid linear pipe elements defining the pipeline cross-section, as illustrated in 4.12c. Using smaller circumferential master rollers was in this case necessary to achieve a consistent contact interface and avoid penetration of the pipeline.

Warp Line Bracket

The warp line bracket interaction was modeled using smaller circumferential master roller defining the outer shell of the pipeline and the warp line bracket was modeled with a single linear pipe element. The warp line bracket to pipe interaction is illustrated in figure 4.12d.

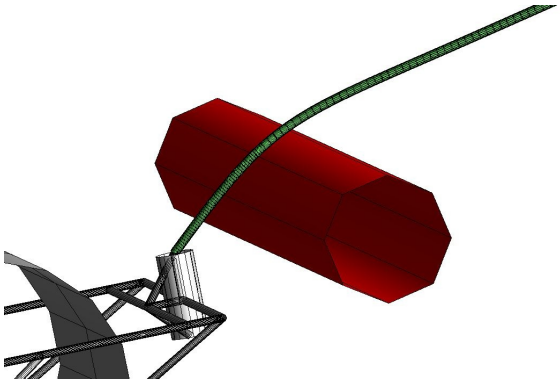

(a) Warp line

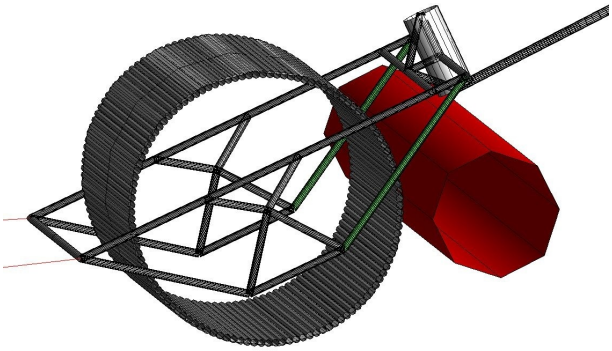

(b) Frame

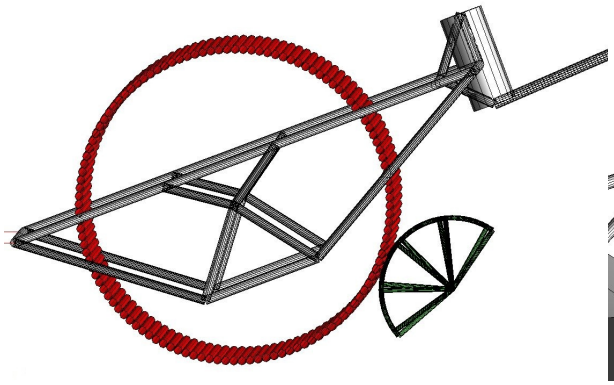

(c) Clump weight roller

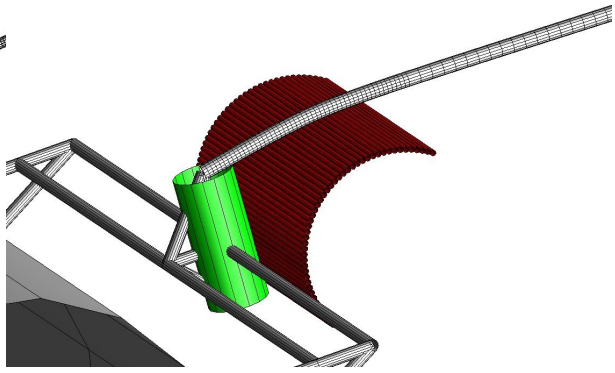

(d) Warp line bracket

Figure 4.12: Illustration of clump weight to pipeline contact interfaces, structural slave elements in green, master rollers in red.

4.4.1 Definition of Contact Interfaces

The contact interfaces are defined using interaction curves in normal, axial and circumferential direction of the master rollers. SIMLA applies these material curves as a penalty stiffness defining the contact interaction. In normal direction a force-displacement curve, depending on penetration of the master roller, is used to represent the normal stiffness. In all simulations and contact interfaces the normal contact stiffness was handled by a force-displacement curve derived from experimental tests, illustrated in figure 4.13,where a 25mm steel rod was forced into the coating of a test pipeline, 280.5 mm in diameter including 18 mm coating, see [13].

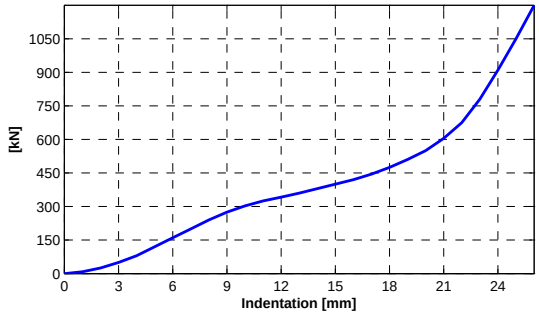

Figure 4.13: Normal stiffness curve for master rollers

The axial and circumferential interaction curve is illustrated in figure 4.14. Friction force is applied by a Coulomb friction model, scaling this curve with the normal contact force and a specified friction coefficient. However during modeling, the obtained simulation result turned out to be completely insensitive to the applied friction coefficient, when varied between 0.0 and 0.8. Various measures were tried without successfully including friction, this is further discussed in 6.1. The simulations have to be regarded as performed without friction in axial and circumferential direction.

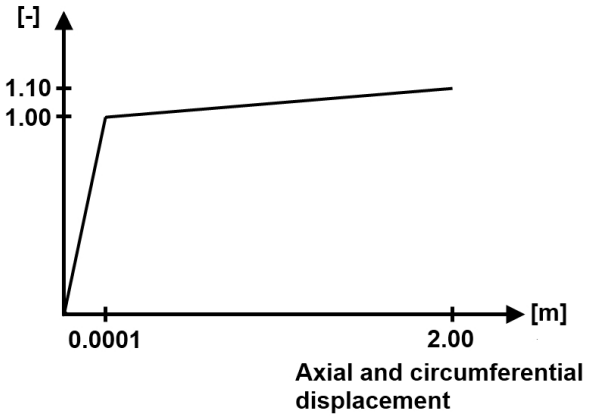

Figure 4.14: Axial and circumferential stiffness curve for master rollers

4.4.2 Contact Definition Philosophy

Defining the normal stiffness has been a reoccurring challenge in previous work done by both Martin T. Møller [14] and Vegard Longva [12] in simulating trawl door pull-over interference in SIMLA, as also the case during this thesis work. Initially, the clump weight was seen to occasionally penetrate the pipeline, leading to the clump weight and pipeline being violently forced from each other in opposite direction, resulting in large peak forces and spurious pull-over behavior.

Vegard Longva ,[12], successfully avoided this contact problem by reducing the slave element size, using overlapping elements and modifying the contact stiffness stepwise during analysis, requiring several restart to carry out a single simulation. Applying these methods turned out not to be sufficient for simulation of clump weight pull-over interference. However the contact problem is believed to be of same origin and was traced to a solely geometrical contact problem in this case. A consistent pull-over interaction was successfully achieved by using a complex contact element arrangement, which proved insensitive to the applied contact stiffness, as long as the contact stiffness was high enough to prevent penetration. The contact element arrangement and contact definition philosophy will be described in detail in this section. It must however be pointed out that this description is mainly based on experience gained during modeling and experimenting with a variety of different contact element arrangements.

The contact elements searches for the corresponding slave elements in an area normal to the master element, as illustrated in figure 4.15a, and it is the slave element center line which must be inside this area in order to determine and establish contact. In addition it was found the center line of the master elements must also be inside an area normal to the slave elements.

Further, the contact search may be improved by applying overlapping elements as illustrated in figure 4.15b.

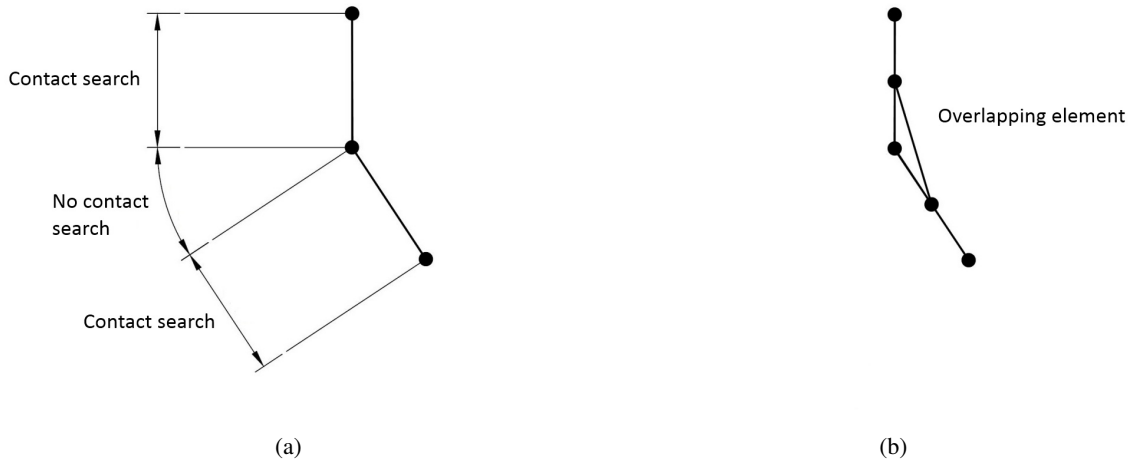

Figure 4.15: Contact search and overlapping elements

The contact definition philosophy is best illustrated with the clump weight roller to pipeline interaction. Initially the clump weight roller was modeled by a single master roller. The master roller were moved to the clump weight to reduce computational time, as contact search for rotating structural elements proved demanding and did not solve the contact problem. Hence 34 overlapping rigid linear pipe elements were used to define the pipeline outer geometry. Contact forces were transferred to the pipeline mid-node by rigid internal beams. These elements were assigned a very low mass in order to not influence the pipeline response. This contact element arrangement, without use of overlapping elements is illustrated in figure 4.16a. In this case, due to the distance between the master roller center line and point of interaction, it is obvious that the master roller will move in and out of the search area as the clump weight is pulled over the pipeline, resulting in loss of contact, penetration and violent response as the contact again is obtained. From this it is also seen that reducing the element size of the slave elements will not solve this problem, only reduce the search area of each element and create more areas were contact is not defined.

This contact problem was solved by using overlapping elements defining the outer pipeline geometry and using smaller circumferential master rollers to define the outer geometry of the clump weight roller, as illustrated in figure 4.16b. In this case the master rollers will move in a continuous search area and the point of interaction will be defined during the entire pull-over. The same principle was also used in defining the warp line bracket to pipeline contact interface.

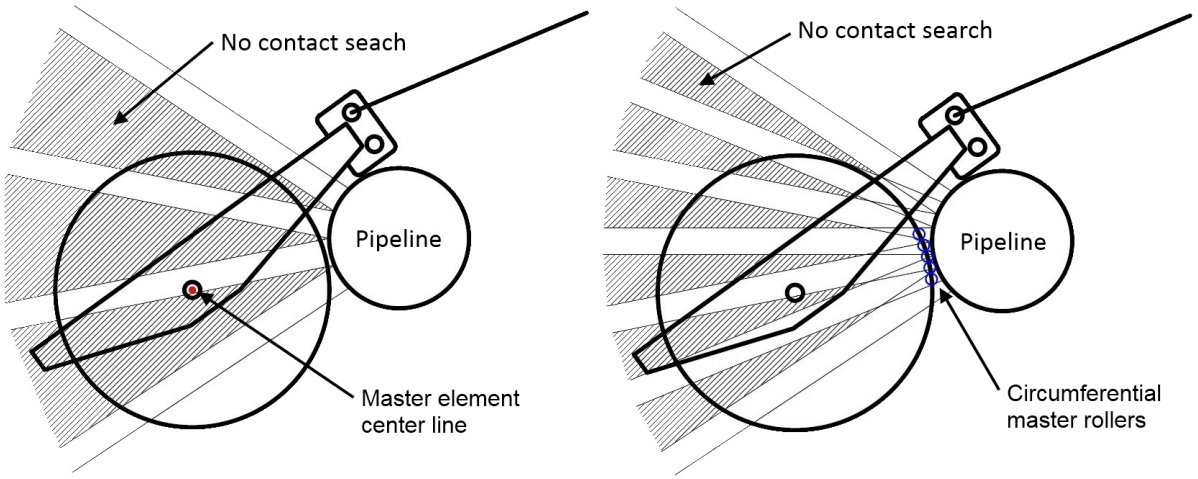

(a) (b)

Figure 4.16: Contact search area

4.5 Estimation of Damping

4.5.1 Contact Damping

Local eigenfrequency damping is used to estimate the contact damping, which was applied between the clump weight and pipeline, clump weight and seabed and pipeline and seabed. The damping coefficient is calculated considering local mass, added mass, and the applied normal contact stiffness, according to,

$$C = 2\lambda\sqrt{(m + m_a) \cdot k_c} \tag{4.1}$$

where C is the damping coefficient, λ is the damping ratio and k_c the normal contact stiffness.

For the clump weight to pipeline interaction only the mass and added mass of the clump weight were included in the eigenfrequency calculation. The contact stiffness was taken as the linear slope of the lower part of the force-displacement curve illustrated in figure 4.13. The damping ratio was set to 5% of critical damping.

Seabed contact damping was calculated considering pipeline and clump weight mass per meter. The contact stiffness was taken as the slope of the force-displacement curves given in figure 4.11. For the pipeline to seabed interaction the damping ratio was set to 5% of critical damping. For the clump weight to seabed interaction a damping ratio of 7% was applied to assure a steady clump weight behavior during towing, as this interaction does not contribute to the pull-over response.

4.5.2 Structural Damping

Rayleigh damping is used to include structural damping in the model. The damping force is defined proportional to the mass matrix **M** and stiffness matrix **K**. Constants α_1 and α_2 are used to define the magnitude of the structural damping. The term proportional to mass and the term proportional to the stiffness will damp out low and high frequency oscillations respectively [11].

$$\mathbf{C} = \alpha_1\mathbf{M} + \alpha_2\mathbf{K} \tag{4.2}$$

No mass proportional damping was applied, α_1 = 0. To avoid high frequency oscillations and unnatural behavior in the simulations stiffness proportional damping was applied. A sensitivity study was performed in order to determine the α_2-parameter. Maximum horizontal pull-over force versus α_2 is plotted in figure 4.17.

The simulations were carried out with the free spanning pipeline model and a 0.5m span height. The α_2-parameter was initially assumed equal to 0.095 and was varied between 0.02 and 0.16. However, in some of the simulations a contact problem occurred as the clump weight penetrated the seabed during interaction. Due to the high contact stiffness applied both to the seabed and pipeline, the clump weight was unnaturally pushed back and forth between the seabed and pipeline, resulting in the pipeline being displaced and the clump weight pulled more easily over the pipeline. The contact problem is illustrated in Appendix C. These simulations are represented with blue markers in figure 4.17. Disregarding these simulations, too low stiffness proportional damping resulted in unnatural oscillations of the clump weight and hence the clump weight was pulled more easely over the pipeline. Increasing α_2 reduces the oscillations and the pull-over duration and force increase. A plateau in the maximum horizontal force was obtained between 0.06 and 0.14, indicating that a sufficient magnitude of damping is applied. The α_2-parameter was kept at 0.095.

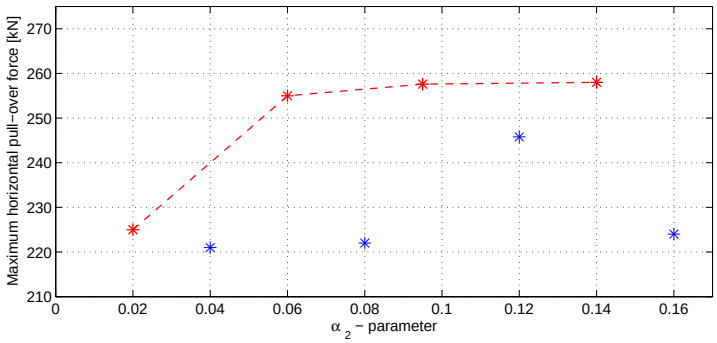

Figure 4.17: Maximum horizontal pull-over force vs α_2-parameter

4.6 Application of Added Mass

Added mass for a cylinder in heave and sway in infinite fluid is equal to the mass of water displaced by the cylinder [6]. SIMLA applies added mass to each pipe element according to

$$m_a = C_a \pi \rho r^2 l \tag{4.3}$$

where C_a is the added mass coefficient and l is the pipe element length. In infinite fluid C_a is equal to 1.0, in immediate proximity to a wall or in this case the seabed, C_a is equal to 2.29 [6]. However, during modeling it was discovered that the current version of SIMLA applies an added mass coefficient equal to 1.0 by default. To account for seabed proximity for the clump weight and the part of the pipeline resting on the seabed it was necessary to apply added mass in two contributions, $1.0\pi\rho r^2$ was included by default and $1.29\pi\rho r^2$ applied as additional structural mass to both the clump weight and pipeline.

4.7 Description of the Simulation Procedure

At the start of the analysis the clump weight is situated 20 m from the pipeline. The clump weight roller and frame are initially fixed towards rotation and a static analysis procedure is applied the two first seconds of the simulation. During the first second, static loads such as gravity and external pressure are gradually applied. At 1.0 s the towing node starts to accelerate and the warp line is tensioned. At 2.0 s the analysis is stopped, the fixation of the clump weight roller and frame removed, and the analysis restarted. From here on, a dynamic analysis is performed. The towing node is gradually accelerated until a towing velocity of 1.95 m/s is obtained after 10 s. After this the clump weight is towed at a constant velocity. A constant drag resistance and backtension from the trawl nets are achieved at 15.0 s, about 1-2 s before the clump weight interferes with the pipeline.

In all simulations, the dynamic analysis is performed with a concentrated mass representation of all structural elements. Unbalanced inertia, damping and internal forces are handled by a displacement based convergence criterion, with a tolerance of 10^{-5} for each equilibrium iteration, as recommended in the SIMLA Manual [18]. Time steps in order of 10^{-2} s was necessary to obtain an appropriate number of equilibrium iterations during towing and acceleration of the clump weight, 10^{-3} during interference. The CPU-time of the simulations varies between 10-20 minutes on a medium-end laptop. The experimental test model with the shortest pull-over duration is less demanding, whereas the free spanning pipeline model is to some extent more demanding. Simulations with a complete set of contact interfaces were approximately carried out in 45 minutes.

4.8 Sampling of Pull-over Forces

Due to complexity and number of contact elements used to model the clump weight interference, it was not practically possible to extract the pull-over forces directly as contact forces between each master and slave element. Pipeline shear forces at the two closest nodes to the midspan node have been sampled instead and the sum taken as the pull-over force. The sampled element shear forces are given according to the local element coordinate system; hence, as the pipeline is displaced in bending, the elements are rotated compared to the global coordinate system. This will induce a discrepancy in sampling of pull-over forces as some of the pull-over force will be taken up as an axial contribution during interference. In addition inertia and drag forces along the element will reduce the sampled shear force.

The element length at mid span was for that reason initially chosen small in order to reduce the discrepancy. The axial contribution was expected to be small and correcting the sampled shear forces for the axial contribution was considered too time-consuming, requiring a lot of manual post processing. The pull-over force histories presented in Chapter 5 are hence presented as the sum of shear forces obtained from the elements closest to the mid node.

To verify sampling of local element shear forces instead of sampling global contact forces, three simulations with 0.5 m span height, applying the DNV pull-over point load for a 0.25m span height, were carried out and compared to the sampled sum of shear forces. The applied force-time history is the same as given in Section 2.3, where maximal horizontal force is 287.9 kN and upward vertical force is 62.4 kN. As the axial contribution is more pronounced at large pipeline deflection, this load history will be conservative compared to all results obtained with the clump weight contact model presented in Chapter 5. Two simulations were carried out with the rigid experimental test model, including fixed and flexible end condition. One simulation was carried out with the free spanning pipeline model. The obtained sum of element shear forces is given below.

Pipeline model	**Maximum horizontal shear force kN**	**Maximum vertical shear force kN**
Rigid pipeline, fixed	286.4	61.6
Rigid pipeline, flexible	286.4	61.5
Flexible pipeline model	281.5	61.1

Table 4.8: Sampled shear forces at midspan

For the rigid pipeline model with fixed end conditions the discrepancy is 1.5 kN in horizontal direction and 0.8 kN in vertical direction. The same discrepancy is observed using flexible end conditions, allowing the pipeline to move, which indicates that contribution from inertia and drag forces over an element length of 0.25 m is insignificant. When using flexible free spanning pipeline model the pipeline is in addition allowed and to bend during interference. Here a 6.4 kN and 1.3 kN discrepancy was obtained in horizontal and vertical direction respectively, assumed mainly caused by the axial force contribution. Thus, shear force sampling gives an adequate representation for the rigid pipeline used in the experimental test model. For the flexible free spanning model the discrepancy is low, resulting in a 2.2% lower maximum horizontal pull-over force compared to the applied point load in horizontal direction.

Chapter 5

Results

Various simulations have been carried out to investigate pull-over forces on free spanning pipelines. Both the experimental test model, initially created for verification purposes, and the free spanning pipeline model have been used for this purpose. The two models are described in Section 4.2.1 and 4.2.2. The experimental test model have been used to isolate and investigate the effect of lateral pipeline flexibility and the free spanning pipeline model used to investigate the effect of including both lateral and vertical flexibility. In addition simulations regarding clump weight center of gravity, varying warp angle and warp line attachment point have been performed to investigate how the pull-over force is affected by the clump weight design and trawling configuration.

In all simulations the clump weight is towed perpendicular across the pipeline. The clump weight is restrained from translation in lateral direction, rotation in the horizontal plane and axis of towing direction i.e. the clump weight will always hit the pipeline level and parallel to the pipeline. The clump weight roller was modeled including spin and left rotating undisturbed during interference. Interference occurs at mid-span and all interaction forces from the clump weight are transferred to the pipeline mid-node.

The pull-over interference was found to be governed by the warp line and warp line bracket interaction, as the clump weight is stopped and rotated or lifted over the pipeline about this point. When released from this position, onset of maximum pull-over force has occurred and the accumulated warp line tension will rapidly pull the clump weight up and away from the pipeline. For that reason only the warp line and warp line bracket contact interfaces were included in the simulations. Interaction with the frame or clump weight roller may only occur at the late end of the pull-over phase and may be considered as a second impact, resulting in peak forces in the pull-over force history. The difference between using only the warp line and warp line bracket interfaces, relative to a full set of contact interfaces, are for comparison illustrated in Appendix D. However, it should be mentioned that a full set was applied when lowering the warp line attachment point, as presented in Section 5.4.4.

Both horizontal and vertical pull-over force are given as force-time histories in the following sections. Vertical pull-over force is defined positive acting upwards. For comparison the pipeline mid-node displacement is also included. The pull-over forces have been obtained from sampling element shear forces at pipeline mid-span. As explained in 4.8, sampling of shear forces will induce a discrepancy due the axial force contribution when the pipeline deflects. This discrepancy is largest for increasing deflections, hence negligible for all simulations with the rigid experimental test model. For the flexible free spanning pipeline model the discrepancy is regarded to be small, as an upper bound estimate the sampled maximum pull-over force may be considered 2.2% higher due to the axial force contribution.

The simulation results proved insensitive to applied contact friction between the clump weight and pipeline. No differences in pull-over forces were observed varying the friction coefficient, hence the simulations have to be regarded as performed without friction. Various efforts were tried to include friction without success, this is further discussed in Section 6.1.

It must also be mentioned that the seabed contact problem described in Section 4.5.2 and illustrated in Appendix C was only present in some of the simulations results presented in this chapter. However, the extent of this contact problem was very limited and did not influence the obtained results in these cases.

5.1 Clump Weight Behavior

The clump weight have been found to behave quite similar in all of the simulations carried out, both for the rigid experimental test model and flexible free spanning pipeline model. In general the pull-over interference can be divided into five steps.

1. First the warp line interacts with the pipeline; the clump weight is lifted from the seabed floor due to the backtension from the trawl nets.
2. The warp line bracket impacts the pipeline, backtension and clump weight forward momentum are lost.
3. The clump weight settle at a lower position relative to the pipeline, with the clump weight stuck in this position, the warp line is tensioned and the clump weight and pipeline are pulled along the seabed.
4. As the pipeline deforms and pipeline resistance increases, the clump weight is gradually lifted vertically or rotated from this position.
5. Finally the clump weight is able slide over the pipeline, and due to large tension forces accumulated in the warp line the clump weight is rapidly pulled up and away from the pipeline.

To illustrate the different stages during interference, screen shots from simulation for 0.75m span height with the free spanning pipeline model are given in figure 5.1. The clump weight behavior is similar for 0.5m span height scenarios, however for 0.25m span height scenarios the warp line will in general clear the pipeline and the warp line bracket hit the pipeline directly.

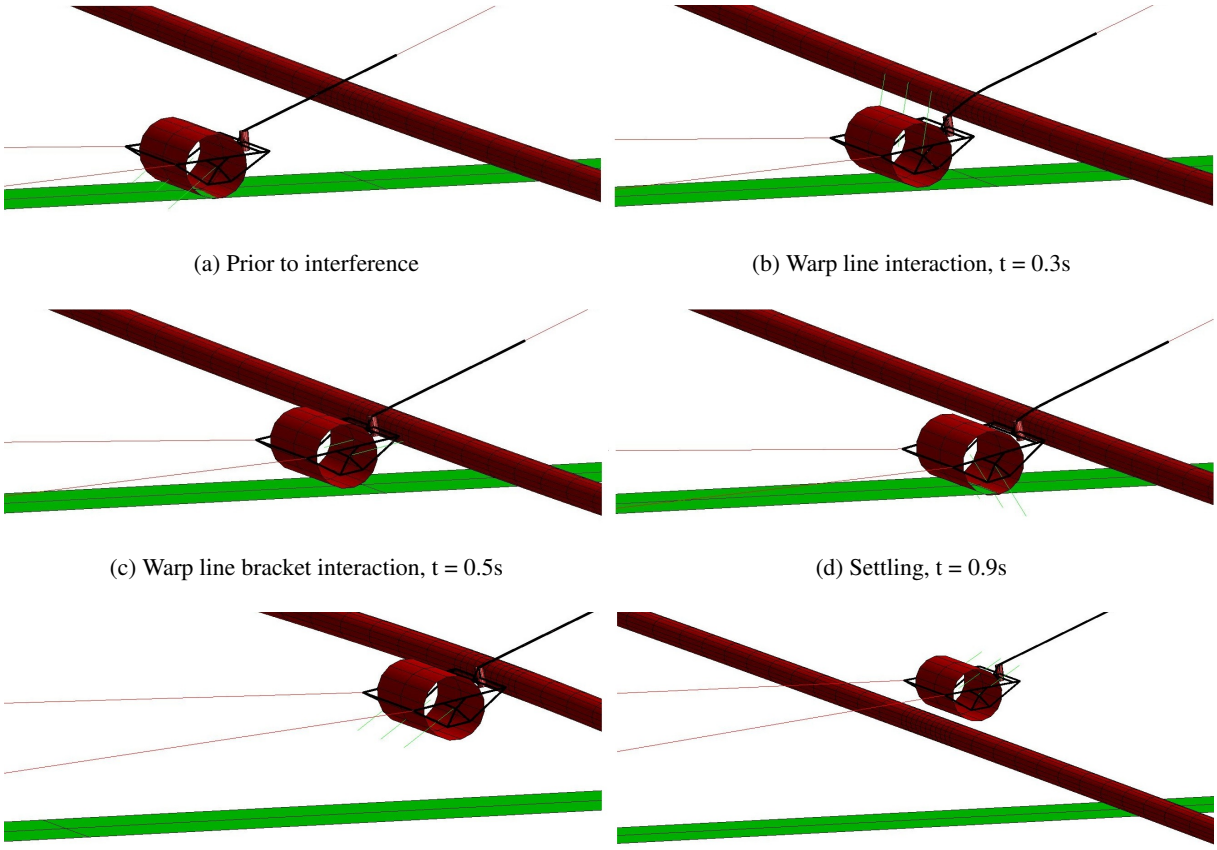

(a) Prior to interference

(b) Warp line interaction, t = 0.3s

(c) Warp line bracket interaction, t = 0.5s

(d) Settling, t = 0.9s

(e) Tensioning of the warp line, t = 6.3s

(f) Release, t = 6.8s

Figure 5.1: Clump weight pull over behavior

In most of the scenarios a combination of lift and rotation of the clump weight was observed. From simulation, increasing pipeline stiffness seemed to favor rotation, while lower pipeline stiffness seemed to favor lifting of the clump weight. By considering vertical equilibrium and momentum equilibrium about the point of interaction, neglecting backtension and dynamic effects, the clump weight behavior during pull-over may be considered analytically to illustrate the governing of these to interaction modes.

As illustrated in figure 5.2, neglecting friction, the clump weight will start to lift when the vertical force component of the warp line is greater than the downward acting force of the clump weight,

$$F_{w,z} > mg \tag{5.1}$$

where $F_{w,z}$ is the vertical warp line force component and mg is the weight of the clump weight.

The clump weight will start rotate about the point of interaction when rotational moment from the warp line is greater than the rotational moment from the clump weight, assuming that friction is sufficient to prevent the clump weight from sliding,

$$F_w \cdot r_w > mg \cdot r_c \tag{5.2}$$

where F_w and mg is the warp line force and weight of the clump weight respectively, r_w and r_c is the warp line and clump weight moment arm about point of interaction, respectively.

The clump weight rotational arm will increase as the clump weight is rotated, hence the pull-over may be initiated by rotation, before lifting and sliding prevails. The lesser of these two expressions given above may also be considered as an indication of the minimum static warp line force needed in order to turn the clump weight over the pipeline, hence also an indication of the corresponding minimum pull-over force exerted to the pipeline during pull-over.

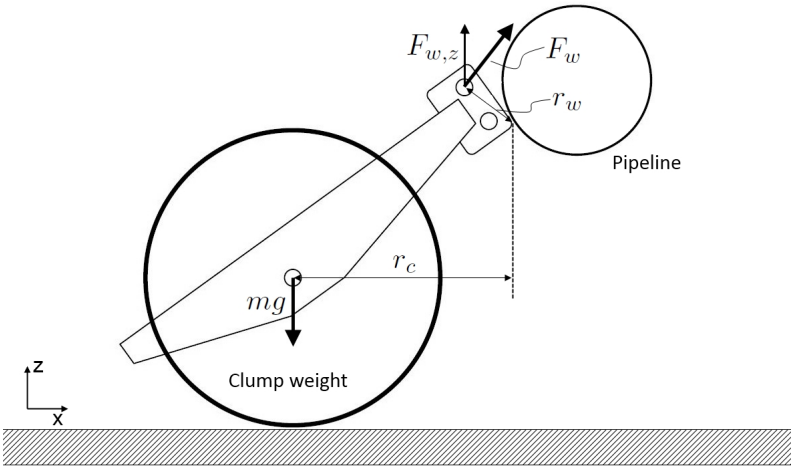

Figure 5.2: Clump weight pull-over response

5.2 Global Pipeline Response

The typical pipeline response from simulation with the flexible free spanning pipeline model is described in this section. The same 0.75m span height scenario used to illustrate typical clump weight behavior is here used to illustrate the corresponding pipeline response at the different stages during pull-over. Lateral pipeline displacement is illustrated in figure 5.3 and mid-span vertical displacement is illustrated in figure 5.4.

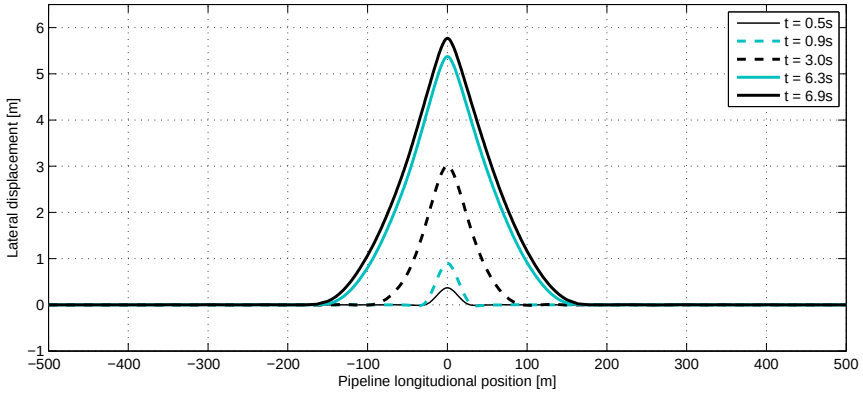

Figure 5.3: Lateral pipeline displacement during pull-over

From figure 5.3, lateral pipeline displacements are observed mainly caused by temporary hooking of the clump weight as the warp line is tensioned. The ability to resist clump weight interaction is in general governed by pipeline bending resistance, mass inertia forces, drag forces, soil resistance and geometrical stiffness, or accumulation of membrane forces as the pipeline deflects. For the 350mm small diameter pipeline, in empty condition, bending resistance, mass inertia forces, drag forces will be low; hence large deflection occur until accumulated membrane forces is able to resist the clump weight interaction.

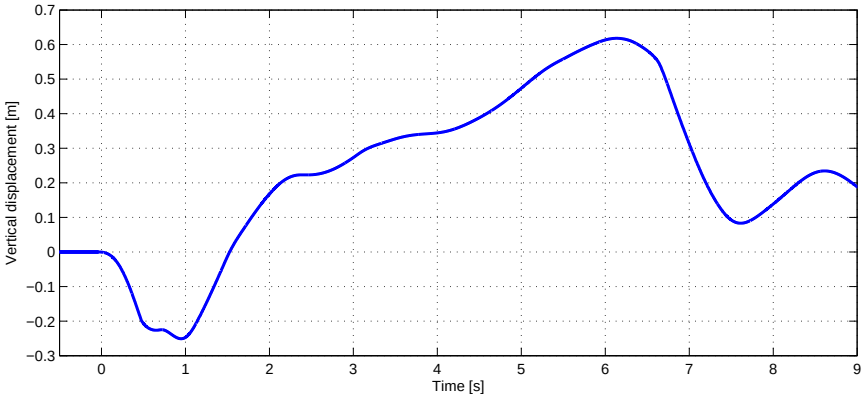

Figure 5.4: Vertical pipeline displacement during pull-over

From figure 5.4, the pipeline is first pulled down by the warp line and the weight of the clump weight when settling. After about 0.9s the warp line starts to tension and the pipeline is gradually lifted until the clump weight is released.

5.3 Experimental Test Model

5.3.1 Verification of Contact Model

An overall objective in this thesis has been to create a contact model able to give a correct representation of the clump weight pull-over phase. Experimental test data have been made available in order to verify the SIMLA model. A total of six different tests have been simulated and compared. Primarily horizontal pull-over forces have been used for comparison. For test no. 3281 plots of vertical pull-over force, warp line tension and horizontal displacement have also been available. Span height and pipe end condition was varied between the different simulations, where the pipe end condition was either fixed or flexible. The different test configurations are given in the table below.

Test no.	**Tow Velocity** m/s	**Pipe Diameter** mm	**Span Height** m	**Pipe end condition**	**Spring Stiffness** kN/m	**Damping** kN/s	**Warp line stiffness** kN/m
3100	1.95	350	0.25	Flexible	40	5	30
3120	1.95	350	0.25	Fixed	40	5	30
3190	1.95	350	0.50	Flexible	40	5	30
3210	1.95	350	0.50	Fixed	40	5	30
3281	1.95	350	0.75	Flexible	40	5	30
3300	1.95	350	0.75	Fixed	40	5	30

The trawl gear configuration was kept unchanged in all simulations. The pipeline was modeled totally rigid to account for scaling effects and span height was varied by adjusting the vertical position of the pipeline.

As in the experimental tests, springs have been used to represent flexible end condition. The spring stiffness was specified to 40 kN/m in the experimental tests. However, during simulation, a pretensioning of 80 kN/m was found necessary to achieve pipeline displacements of correct order. This may be justified as some initial pretensioning was also present during testing, as explained in section 7.2.

In general, the horizontal pull-over force and duration showed very good agreement with the test results. The magnitude of the initial impact indicates that the applied clump weight model was modeled correctly regarding impact energy, or more specific, velocity of the clump weight prior to interference and assumptions made upon mass and added mass properties. The slope during tensioning of the warp line indicates that the applied warp line configuration is sufficient, reference is made to figure 2.11a. The maximum force or time of release indicates that the simplified modeling of clump weight geometry and mass distribution is sufficient.

In the following, simulations results are compared to experimental test results. Test no. 3281 is presented including vertical pull-over force, warp line tension and horizontal displacements, in addition to horizontal pull-over force in figure 5.5. Further, horizontal pull-over force is compared for three different span heights and either fixed or flexible end conditions in figure 5.6, 5.7 and 5.8.

Comparison with Test no. 3281

Test no. 3281 was performed with a 0.75m span height and flexible end conditions. The obtained horizontal pull-over force is in good agreement with the test result, considering the initial impact at about 0.8s, somewhat higher during tensioning of the warp line from about 2.0 s and maximum horizontal force pull-over force. The drop in horizontal pull-over force between 1-2 s is due to settling of the clump weight. Fall time in pull-over force is shorter in the simulation compared to the experimental tests. This is however also observed in test no. 3190 with flexible end conditions, illustrated in figure 5.7a. The distinct curve during fall time for the flexible cases are believed caused by the clump weight roller and frame impacting the pipeline when released, as illustrated in the filtered results in Appendix D, were

a complete set of contact interfaces was applied for 0.5 m span height and the free spanning pipeline model.

The vertical pull-over forces are however somewhat higher during the entire pull-over, 54% larger at maximum pull-over force. However, the vertical pull-over force is small compared to horizontal pull-over force and is for that reason not so decisive for the overall pull-over response. The discrepancy may be explained by the clump weight angle and contact point during tensioning of the warp line, geometrically resulting in a larger vertical force component compared to the experimental test. The vertical force history can be understood as the first peak at 0.5s is due to the warp line pushing down on the pipeline, second peak at about 0.8s from the clump weight hitting the pipeline at an angle pushing upward on the pipeline. From here on the forward momentum is lost and the warp line is tensioned until the clump weight is pulled over.

Warp line tension is in good agreement and 3.4% larger for maximum force. Regarding pipeline displacement, some differences at the beginning and oscillations after the pull-over are observed. This can most likely be explained by modeled pipe end stiffness and the possibility that the applied damping is different from experimental tests. Overall the maximum horizontal displacement is 9.7% lower compared to the experimental test.

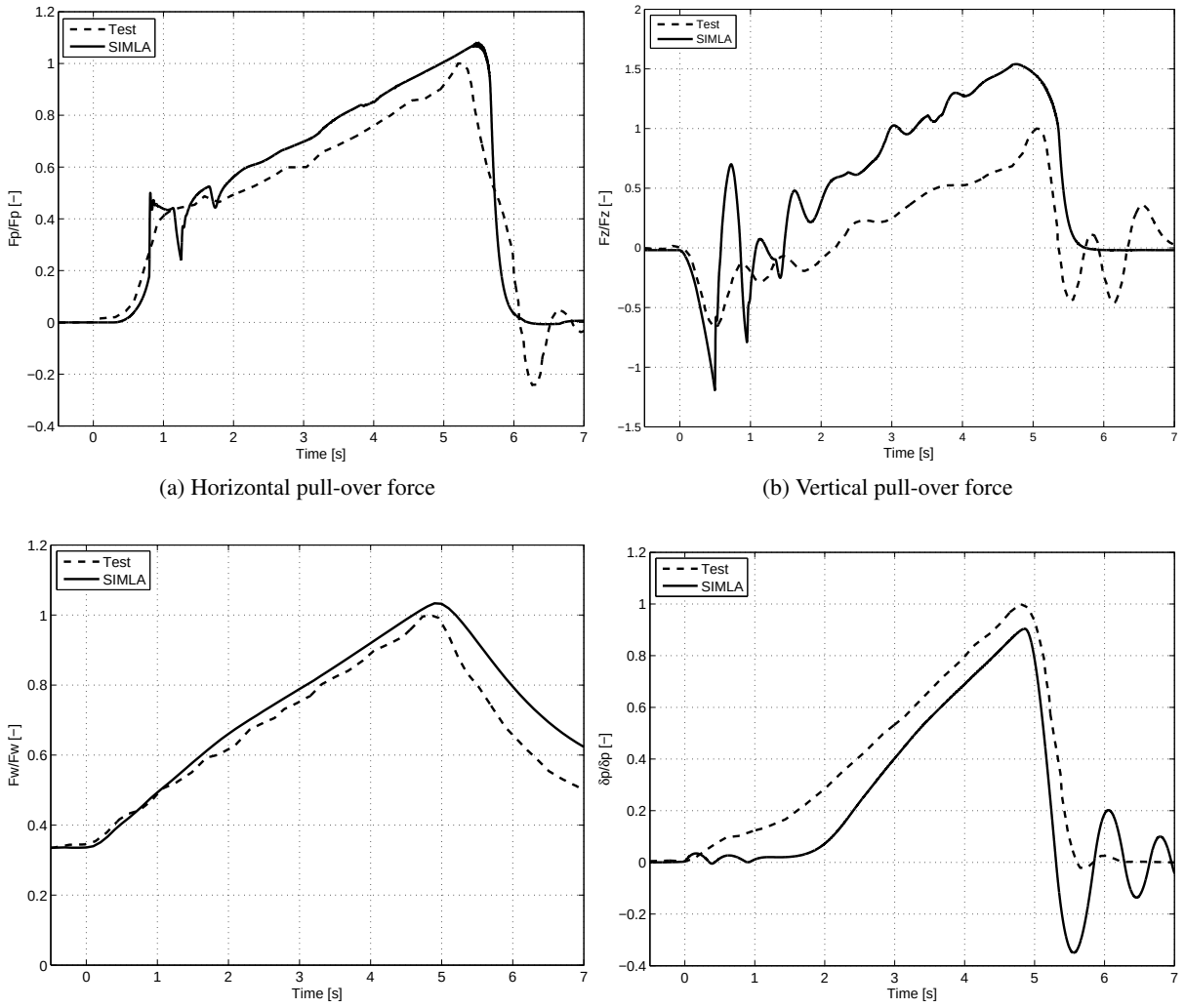

(a) Horizontal pull-over force

(b) Vertical pull-over force

(c) Warp line tension

(d) Horizontal displacement

Figure 5.5: Test no. 3281 - Flexible

Comparison of Horizontal Pull-over Force at 0.75 m Span Height

At 0.75 m span height, a good agreement is obtained both regarding horizontal pull-over and duration. The obtained maximum horizontal pull-over force is 8% and 4% larger for flexible and fixed end conditions, respectively.

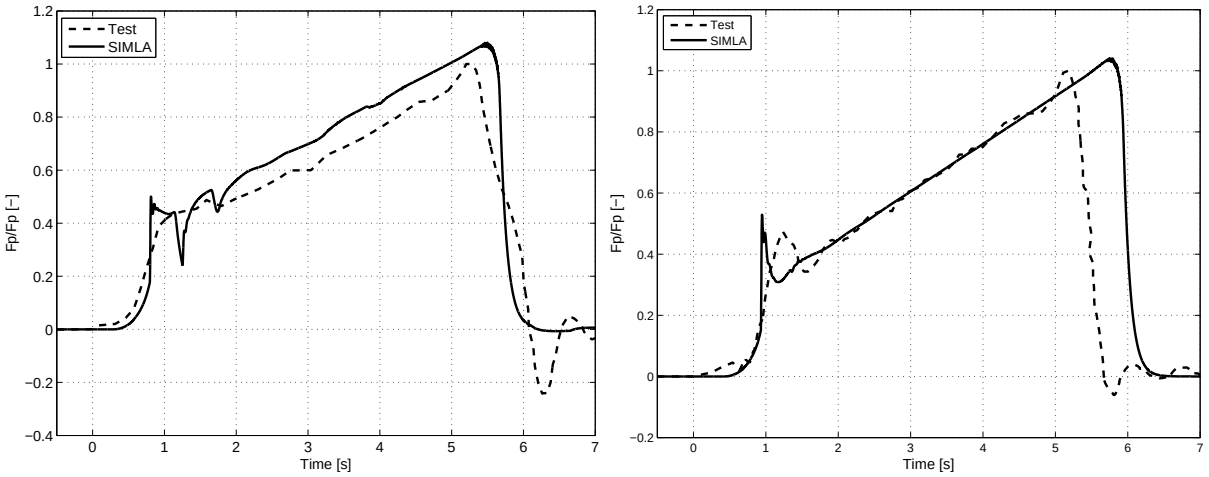

(a) Test no. 3281 - Flexible

(b) Test no. 3300 - Fixed

Figure 5.6: Horizontal pull-over force, comparison with experimental test for 0.75m span height

Comparison of Horizontal Pull-over Force at 0.50 m Span Height

At 0.50 m span height, some differences are observed compared to test 3190 with flexible end condition. The discrepancy in maximum force and duration may however be regarded as a test irregularity. A general trend in the performed tests is that fixed end condition results in larger horizontal maximum force than flexible end conditions. In test no. 3190 the maximum horizontal force is 11% larger than the corresponding 0.5m span height test with fixed end condition. For comparison the 0.25m and 0.75m span height tests with flexible end condition resulted in respectively 8% and 9% lower maximum horizontal pull-over force compared to fixed end condition. For fixed end condition the maximum horizontal pull-over force is about 2% lower compared to the test result.

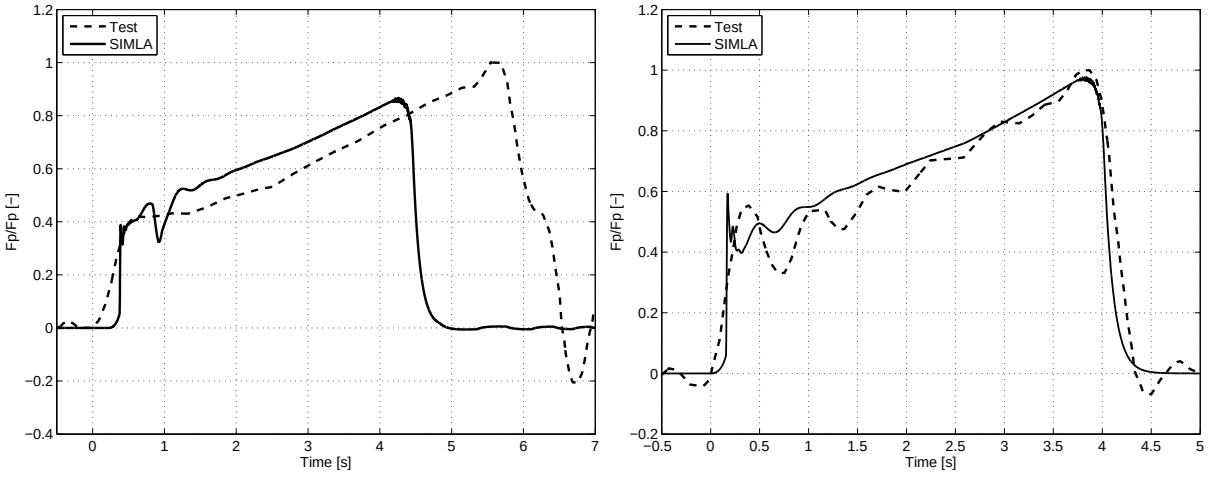

(a) Test no. 3190 - Flexible

(b) Test no. 3210 - Fixed

Figure 5.7: Horizontal pull-over force, comparison with experimental test for 0.50m span height

Comparison of Horizontal Pull-over Force at 0.25 m Span Height

At 0.25 m span height, the difference in maximum horizontal pull-over force is about 2 % in case of flexible end conditions, whereas 20 % in case of fixed end conditions. The duration is about 0.5 s shorter in both simulations. For the flexible case, the discrepancy in duration may be related to only including the warp line and warp line bracket interaction during interference. From simulation, the warp line is in this case to a less extent curved around the pipeline and a more horizontal release of the clump weight is observed. Hence, the clump weight roller and frame interaction may be of greater importance considering lower span heights and flexible pipeline conditions. In case of fixed end conditions at 0.25 m span height, the discrepancy in duration and maximum horizontal pull-over force may be due to seabed interaction in combination with a rigid pipeline interaction resulting in unnatural excitation of the clump weight.

It must however be mentioned that the 0.25 m span height scenarios have been filtered to remove what is believed to be eigenfrequency oscillations during interference. The filtering process and the relative difference between filtered and unfiltered results are briefly described and illustrated in Appendix E. The filtering process is the source of the "negative" horizontal pull-over force during the initiation of the pull-over phase. However, the test results have also been filtered and show the same tendency.

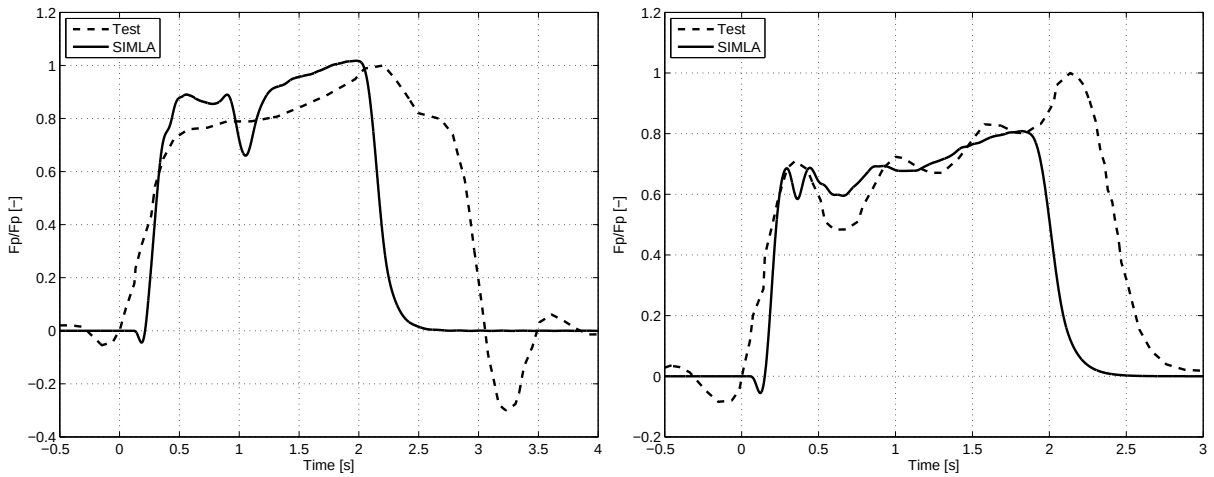

(a) Test no. 3100 - Flexible

(b) Test no. 3120 - Fixed

Figure 5.8: Horizontal pull-over force, comparison with experimental test for 0.25m span height

5.3.2 Effect of Lateral Pipeline Stiffness

The purpose of the simulations presented in this section has been to investigate how the pull-over forces are influenced by increased lateral pipeline flexibility. The simulations were carried out with the experimental test model, illustrated in figure 4.5, which includes a 25m long rigid pipeline section and linear springs at each end to represent pipeline lateral stiffness. The span height was 0.50 m. No pretensioning of the springs was in this case applied and the spring stiffness at each end was varied between 5 kN/m and 40 kN/m. In vertical direction, the pipeline was fixed, hence no vertical displacement was allowed and the obtained result is solely dependent on lateral pipeline stiffness. It must however be pointed out that no considerations have been made regarding whether the applied spring stiffness is representative for a real case.

The obtained horizontal and vertical pull-over histories are presented in figure 5.10 and 5.11. As a reference horizontal displacements are included in 5.12. For comparison, the corresponding DNV pull-over load and a fixed end simulation was also included. In DNV-RP-F111 the pipeline displacement only influences the duration of the pull-over loading, i.e. maximum pull-over force is independent of the pipeline flexibility. Reference is made to section 2.3.3. Here pipeline displacement, δ_p, has been set equal to zero in calculating the pull-over force.

Considering the horizontal pull-over force in figure 5.10, the maximum force is 325.1 kN according to DNV-RP-F111 and 274.7 kN with fixed end condition. The simulation result is hence a factor 0.84 lower than DNV pull-over loading, which is consistent during the entire pull-over. The pull-over duration is the same. According to DNV, the pull-over loading may be reduced with a factor of 0.8 in areas with low trawling frequencies; less than one incident per year [3]. Hence, the difference between the fixed end condition simulation and DNV pull-over loading may be an indication of the inherent safety in DNV-RP-F111.

Regarding the effect of pipeline flexibility, figure 5.10 clearly indicates that a lower lateral stiffness reduce the horizontal pull-over force and increase the pull-over duration. The same result is also obtained in vertical pull-over force. At 5 kN/m pipe end stiffness, a maximum horizontal pull-over force of 172.9 kN was obtained. This is a 37.0% reduction compared to fixed end condition and a 46.8% reduction compared to DNV pull-over loading. This effect is believed related to lower mobilization of mass inertia forces as the clump weight accelerations were found to decrease for increasing pipeline flexibility. Two additional simulations were carried with 2.5 kN/m and 1.8 kN/m pipe end stiffness. Figure 5.9 illustrates maximum horizontal pull-over force versus displacements for the different simulations. The clump weight behavior mode seemed to be governed by pure lifting as the pipeline flexibility increases. In addition, the static horizontal component of the warp line force needed to lift the clump weight was calculated to 122.5kN, as depicted in 5.1, by a simple consideration of submerged weight and a warp angle of 23°.

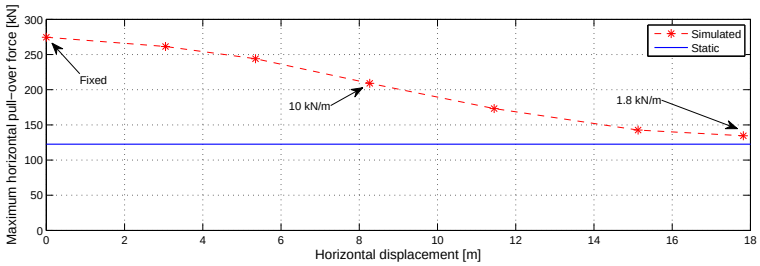

Figure 5.9: Maximum horizontal pull-over force - Effect of lateral pipeline stiffness

As illustrated in figure 5.9 the maximum horizontal pull-over force seems to converge to the static solution of lifting the clump weight over the pipeline. This indicates that a significant difference in dynamic effects are present for rigid pipelines compared to flexible pipelines.

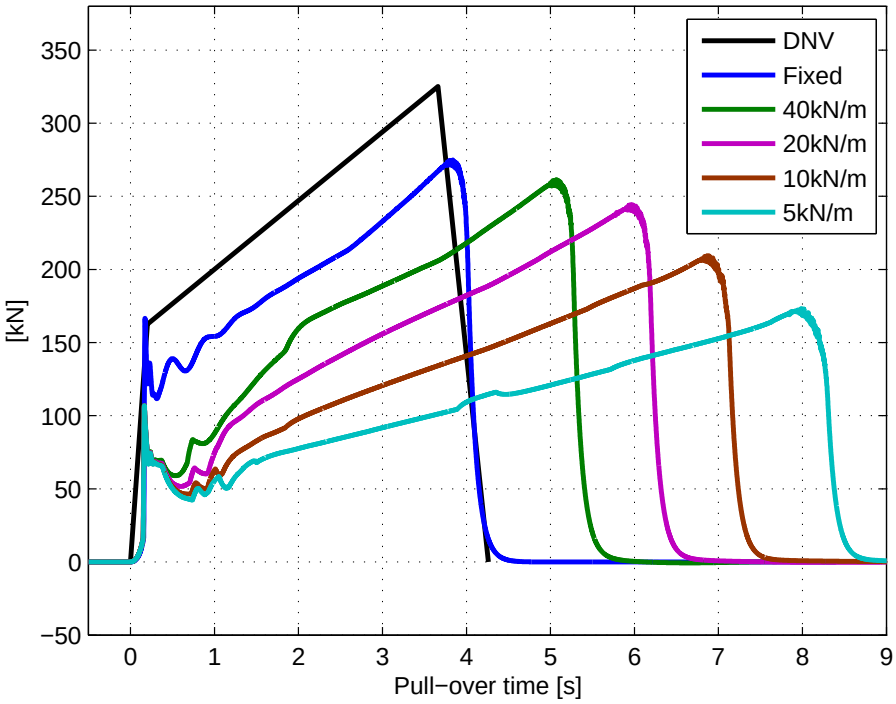

Figure 5.10: Horizontal pull-over force - Effect of lateral pipeline stiffness

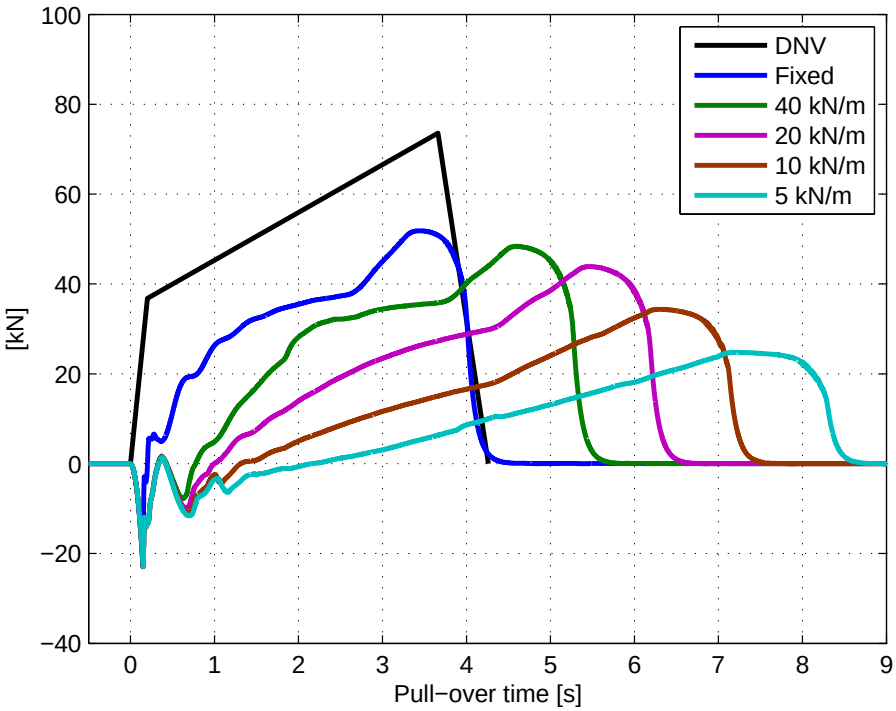

Figure 5.11: Vertical pull-over force - Effect of lateral pipeline stiffness

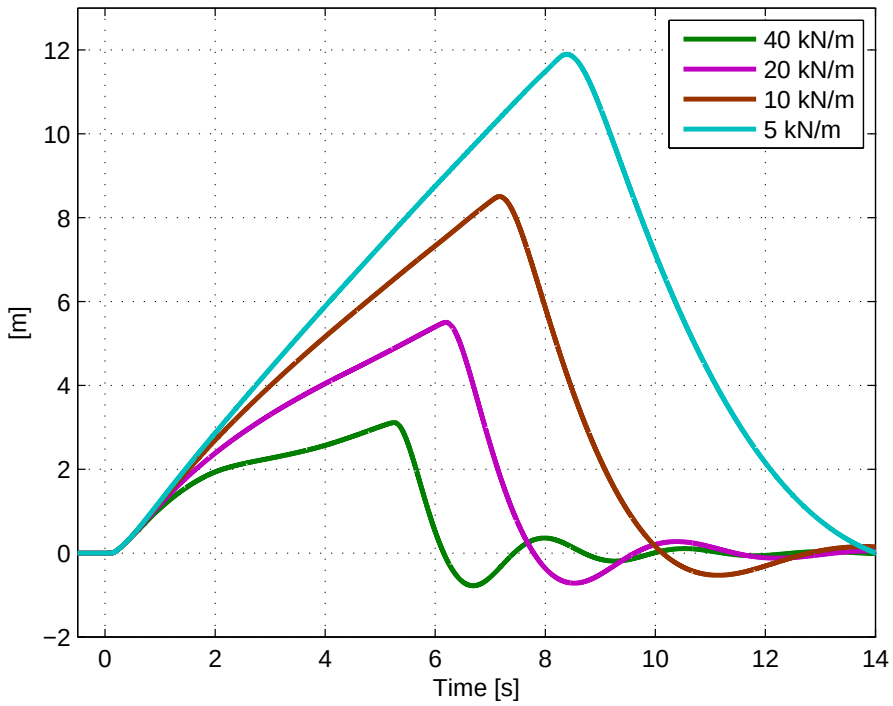

Figure 5.12: Horizontal displacement - Effect of lateral pipeline stiffness

5.4 Flexible Free Spanning Pipeline Model

In this section, the results from simulations carried out with the free spanning pipeline model are presented. The model includes a 1000m long pipeline section, a 50 m free span and realistic soil properties. The trawl gear configuration and pipeline outer diameter have been kept unchanged compared to the experimental test model.

The pipeline was modeled in empty condition, i.e. no content, internal pressure or temperature loading was included. Coating was neglected to be able to perform the simulations at a one to one relationship with the validated experimental test model.

The main objective of these simulations have been to simulate a more realistic pipeline scenario and investigate the pull-over force for a free spanning pipeline considering the effect of both lateral and vertical pipeline flexibility. In addition, with the 0.5 m span height scenario as a base case, the effects of warp angle, clump weight center of gravity and warp line attachment point were investigated.

The pull-over forces obtained from these simulations have been filtered to remove high frequency oscillations. The oscillations occur close to maximum horizontal force and believed caused by temporary loss of contact as the lower edge of the warp line bracket slides over the pipeline.

5.4.1 Effect of Lateral and Vertical Pipeline Flexibility

Simulations for 0.25 m, 0.50m and 0.75m span height were carried out and pull-over forces compared to DNV pull-over loading. The magnitude and duration of the DNV pull-over loading was calculated as described in Section 2.3. An iterative procedure with respect to maximum pipeline displacement was applied to determine the pull-over duration, assuming this to be the most critical load condition. The calculated DNV pull-over loads are given below.

Span height	**0.25m**	**0.50m**	**0.75m**
Maximum horizontal pull-over force	287.9	325.1	344.6
Maximum upward pullover force	62.4	73.6	79.4
Maximum downward pull-over force	37.0	33.3	31.4
Duration	9.57	10.87	11.57

Table 5.1: DNV pull-over load

As illustrated in figure 5.13, the horizontal pull-over force and duration was found considerably lower than the DNV pull-over loading for all span heights. A reduction of 43.5%, 44.4% and 47.4% was observed for span heights of 0.25m, 0.50m and 0.75m, respectively.

As illustrated in figure 5.14, the same effect was also seen in upward pull-over force. A reduction of 57, 1%, 50.0% and 52.5% was observed for span heights 0.25m, 0.50m and 0,75m, respectively. Regarding downward pull-over force, DNV pull-over loading was found to significantly over-estimate the pull-over duration.

The horizontal pipeline displacements are illustrated in figure 5.15. For the 0.50 m span height scenario the maximum horizontal displacement was 5.69 m with a corresponding maximum horizontal pull-over force of 180.8 kN. Compared to the result presented in figure 5.10, varying lateral pipeline stiffness , this corresponds to a pipe end stiffness of 20 kN/m, 5.50 m horizontal displacement and a maximum horizontal pull-over force of 241.2 kN. This is a 60.4 kN or 25% difference, indicating that the vertical pipeline flexibility also have a significant effect on horizontal pull-over forces.

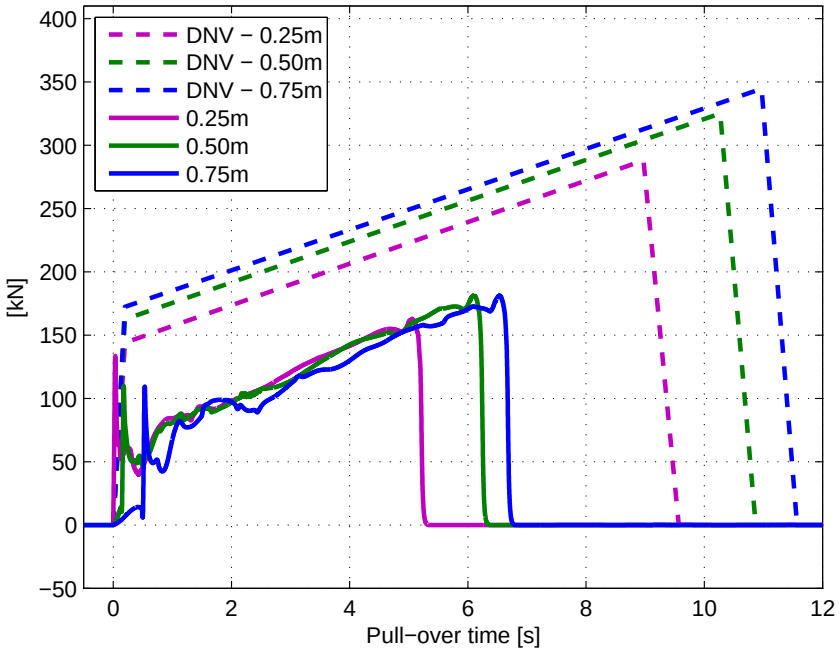

Figure 5.13: Horizontal Pull-over force - Free spanning pipeline

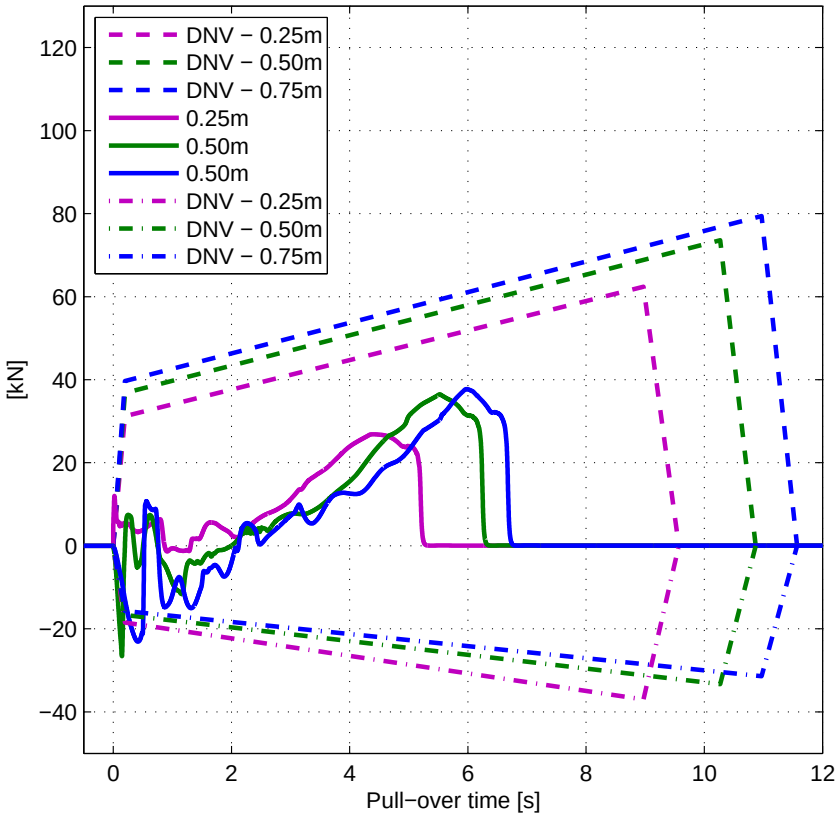

Figure 5.14: Vertical Pull-over force - Free spanning pipeline

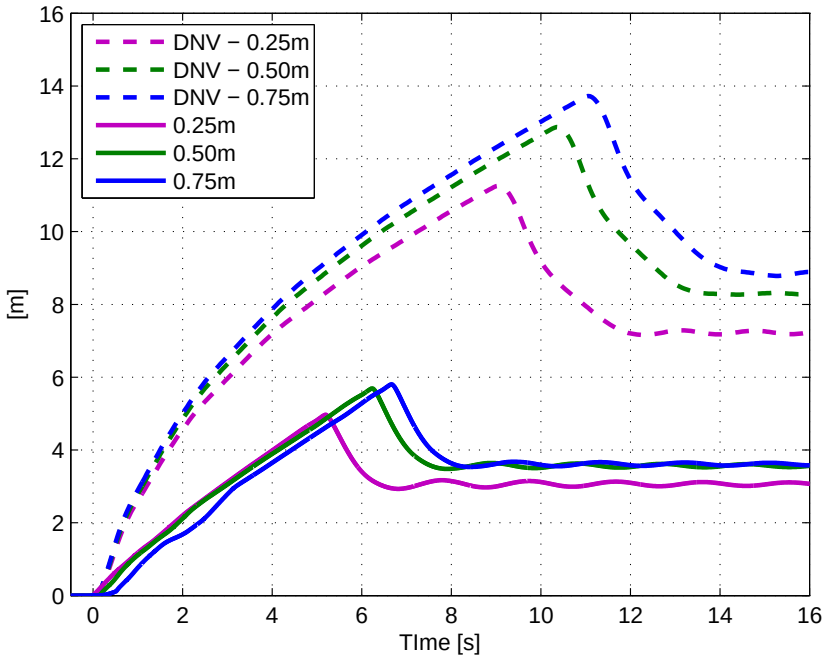

Figure 5.15: Horizontal displacement - Free spanning pipeline

5.4.2 Effect of Warp Angle

In these simulations, the objective was to investigate the effect of warp angle and horizontal pull-over force. Two additional simulations were carried out with a 16.6°and 19°warp angle, compared to 23°for the initial trawl gear configuration. The span height was 0.50 m.

The warp line length is typically between 2.5 and 3.5 times the water depth [3]. In this case, a warp angle of 23°corresponds to a lower bound warp line length of 2.5 times the water depth and 16.6°to an upper bound of 3.5 times the water depth. The effect of different warp line length and stiffness was accounted for by individually adjusting the warp line stiffness to 30 kN/m in all three simulations, hence the obtained result depends solely on warp angle. The applied warp line properties are given bellow.

Warp angle(ϕ) deg	**Length**(l_w) m	**Axial stiffness**(EA) MN	**Length/Depth ratio** -
16.6	1225	37	3.5
19.0	1050	32	3.0
23.0	895	27	2.5

Table 5.2: Warp line properties for varying warp angle

As illustrated in figure 5.16, the maximum horizontal pull-over force decreases for inclining warp angle. From 207.7 kN at 16.6°to 180.8 kN at 23°. This is a difference of 26.9 kN or a 15% reduction from an upper to lower bound warp line length. This may be due to an increase of the vertical warp line force component at larger angles, as illustrated in figure 5.2, which will contribute in lifting or rotating the clump weight over the pipeline. This may also be observed considering the vertical pull-over force in figure 5.17, which in contradiction to horizontal pull-over force, increases for higher inclinations.

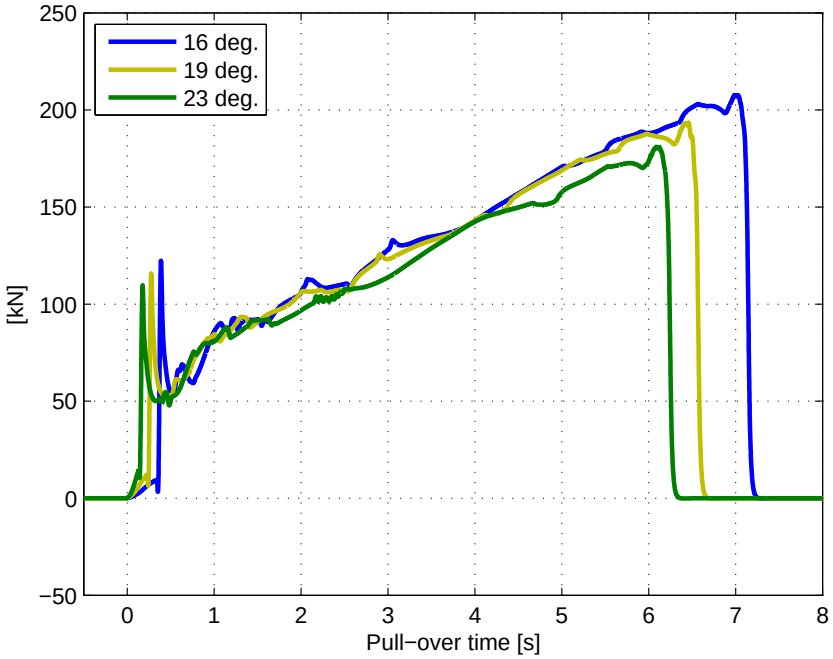

Figure 5.16: Horizontal pull-over force - Effect of warp angle

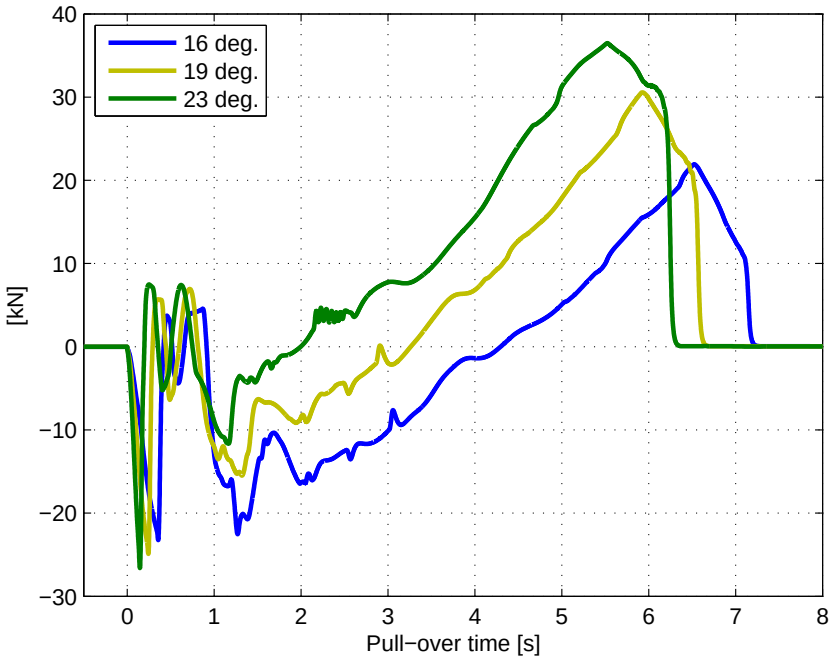

Figure 5.17: Vertical pull-over force - Effect of warp angle

5.4.3 Effect of Center of Gravity

During modeling, the effect of clump weight center of gravity became evident. When the center of gravity was moved forward the necessary moment needed to rotate the clump weight over the pipeline was reduced and thereby lowering the pull-over forces on the pipeline. To illustrate the magnitude of this effect, two simulations were carried out relocating 10% and 20% of the total clump weight mass to the front beam of the frame. The simulations were carried out at a 0.5m free span height.

As illustrated in 5.18, the maximum horizontal pull-over force was in this case reduced from 180.8 kN to 137.6 kN by moving 20% of the clump weight mass. This is a 23.9% reduction and indicates how the pull-over loads are influenced by the clump weight design. When the clump weight is stopped after the initial impact, the mass of the clump weight and distance between clump weight center of gravity and interaction point with the pipeline is decisive for the magnitude of the warp line and pull-over forces. The same reduction is also seen in upward pull-over force illustrated in figure 5.19.

Regarding future clump weight designs this may be an effective way to reduce pull-over loads on both pipelines and trawl gear. However, other factors such as clump weight towing properties and ability to handle uneven and rocky seabed must also be considered and may not favor a more forward center of gravity.

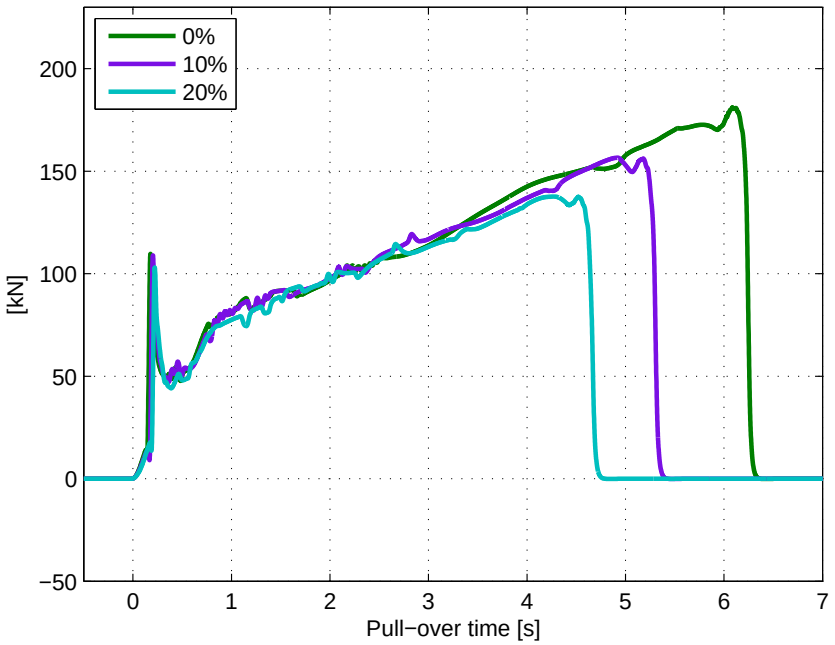

Figure 5.18: Horizontal pull-over force - Effect of center of gravity

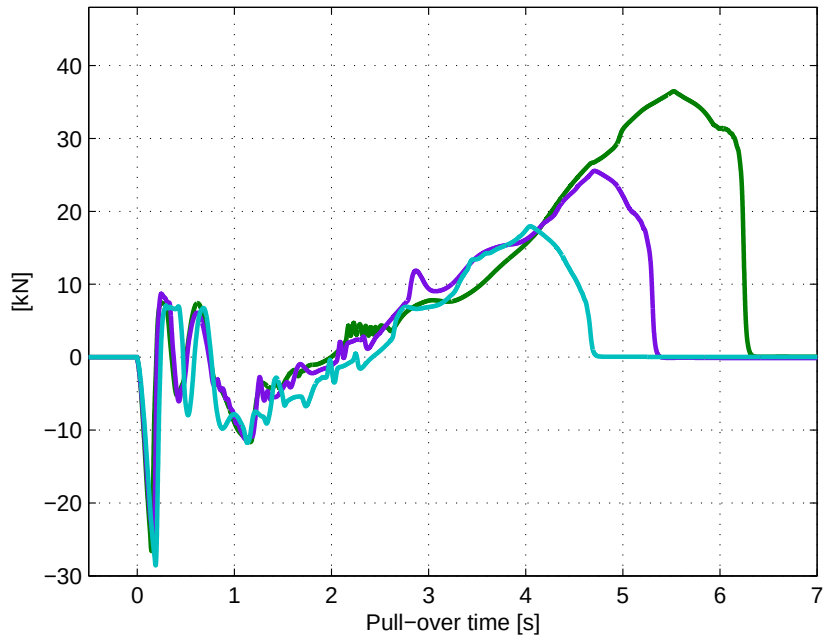

Figure 5.19: Vertical pull-over force - Effect of center of gravity

5.4.4 Effect of Temporary Hooking and Warp Line Attachment Point

Throughout all simulations the pull-over loads was found to be governed by a temporary hooking effect between the warp line, warp line bracket and pipeline. To lift and rotate the clump weight from this position requires mobilization of large warp line forces which further induces large pull-over forces to the pipeline. To investigate the pull-over force if this hooking effect is avoided, a simulation with the warp line attached to the lower point of the warp line bracket was carried out. The span height was 0.5 m and all contact interfaces was applied, including both the clump weight frame and roller interaction. The clump weight model and warp line attachment point are illustrated in figure 5.20. Screen shots from this simulation are given in Appendix F.

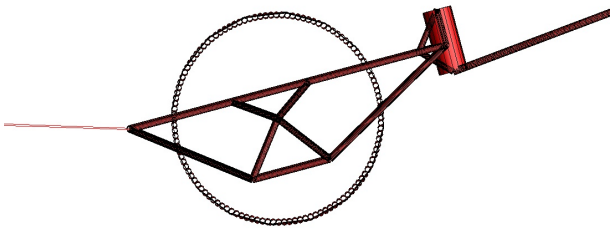

Figure 5.20: Illustration of lower warp line attachment point

The hypothesis was that the clump weight in this case will slide more easily over the pipeline, avoiding temporary hooking at the warp line bracket. It must however be pointed out that the modeling of the clump weight in this case is an idealization to avoid interaction with the warp line bracket. In a real case, the clump weight may still be hooked at the lower corner of the warp line bracket, as illustrated in figure 5.21.

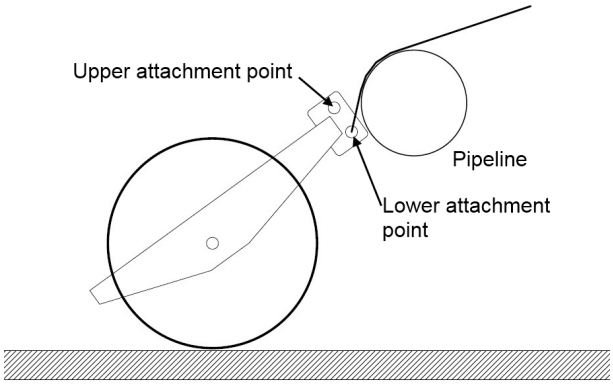

Figure 5.21: Temporary hooking at lower corner of the warp line bracket

As illustrated in figure 5.22 and 5.23, a considerable lowering of both horizontal and vertical pull-over force was obtained. Due to a more uniform sliding motion of the clump weight, the pull-over phase was almost reduced to a case of initial impact. In addition upward acting pull-over forces was avoided completely. It must however be pointed out that friction between the clump weight and pipeline was not included in the model, as sliding occurs, friction may to some degree increase the obtained pull-over forces.

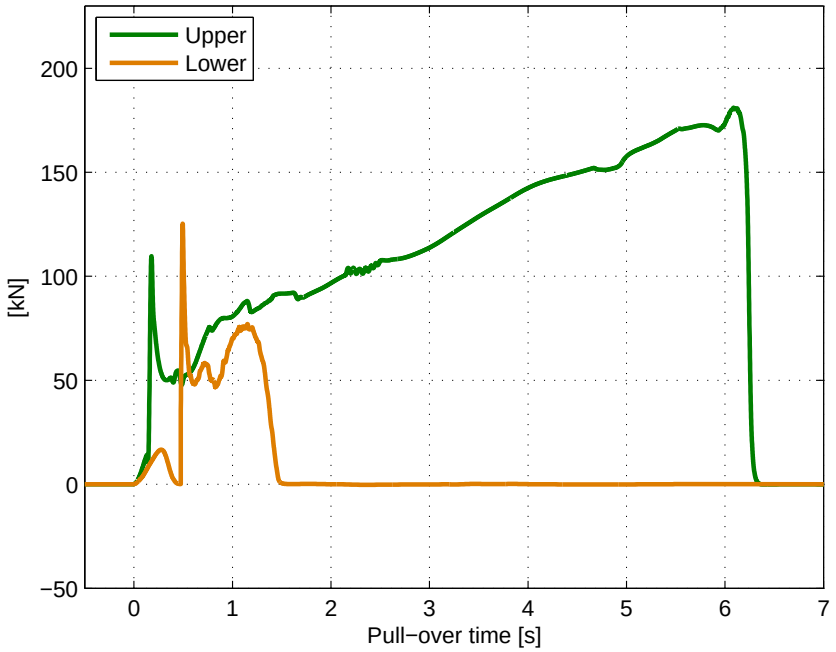

Figure 5.22: Horizontal pull-over force - Effect of warp line attachment point

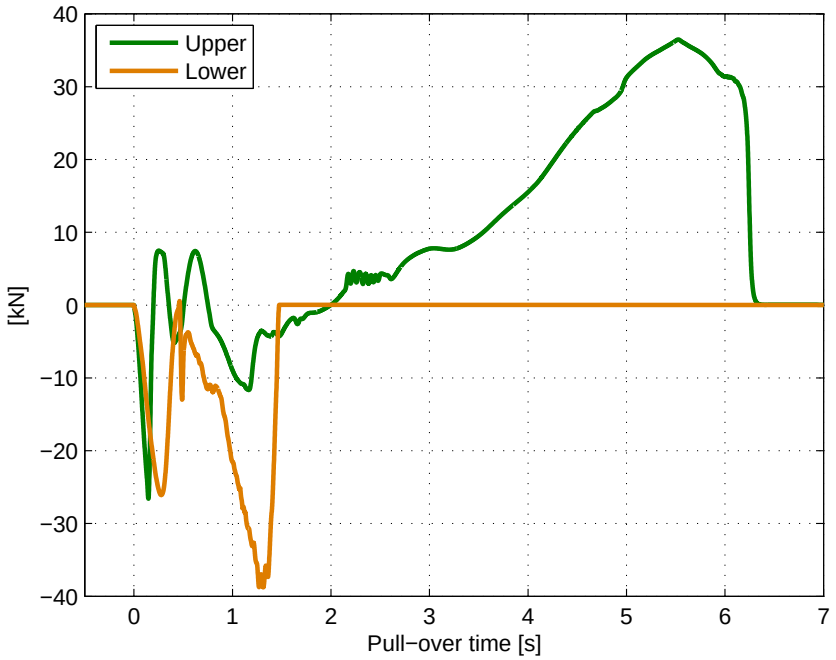

Figure 5.23: Vertical pull-over force - Effect of warp line attachment point

Chapter 6

Conclusion and Recommendations for Further Work

The results from simulation of the experimental tests, presented in section 5.3.1, was found in very good agreement with the test results. This indicates that it its possible to model and simulate clump weight interference with free spanning pipelines, applying a dynamic finite element analysis in SIMLA. More detailed and accurate estimates of clump weight pull-over loads can in this way be obtained and applied in future pipeline designs.

The pull-over loads was found to decrease for increasing pipeline flexibility. This was the case for both horizontal and upward vertical pull-over force. The pull-over duration was however found to increase. This may indicate that significant dynamic load effects are present for rigid pipelines compared to flexible pipelines. This is in contradiction to DNV-RP-F111 which states that the the clump weight response can be represented as a quasi-static load.

The pull-over loads and duration obtained from simulation of a 12" flexible pipeline was found considerably lower than pull-over loads calculated according to DNV-RP-F111. The difference in maximum horizontal and vertical pull-over force was approximately in order of 50% for all three span heights. This is believed to exceede the inherent saftey margins in DNV-RP-F111, however the calulation methos provied within these recommended practice is limited to rigid pipelines. To avoid over-conservatism it is thus reccomended that calculations methods accounting for pipeline flexibility should be developed and applied in future pipeline designs.

Regarding downward acting pull-over force, the maximum force was found in good agreement. However the load shape and duration differ considerably compared to DNV-RP-F111. In all simulations, downward acting pull-over forces was only present during the initiation of interference. DNV-RP-F111 applies a downward acting force during the entire pull-over duration. Thus, as downward acting pull-over forces in general increases soil resistance, which again result in a larger curvature of the pipeline this may influence pipeline response and usage factor.

Three simulations were carried out to investigate the effect of warp angle, applying three different warp line lengths ranging from 2.5 to 3.5 times the water depth. The warp line stiffness was adjusted to 30 kN/m in all three cases. The maximum horizontal pull-over force and duration was found to increase for increasing warp line length and lower inclination of the warp line. The maximum upward pull-over force was however reduced for increasing warp line length. The small scale tests which forms the basis of the calculation methods provided in DNV-RP-F111 was performed with a warp line length 2.5 times the water depth. This may indicate that DNV-RP-F111 could under-estimate pull-over loads for rigid pipelines combined with longer warp line lengths.

The simulations carried out regarding clump weight mass distribution have shown that a more forward center of gravity will reduce both horizontal pull-over force, vertical pull-over forces and duration. The simulation carried out with a lower warp line attachment point resulted in a more uniform sliding motion of the clump weight, avoiding temporary hooking at the warp line. In this case the pull-over loads and duration was almost reduced to a case of initial impact. It is thus suggested that future clump weight designs should reflect this in order to reduce interference loads on both trawl gear and pipelines.

6.1 Further Work

The clump weight pull-over loads was found to be governed by a temporary hooking effect between the warp line, warp line bracket and pipeline as described in Section 5.1. Interaction from the clump weight roller and frame was found of less significance considering free spanning pipelines above 0.25 m span height. Thus, to reduce modeling efforts and computational time in future simulations of interference between roller type clump weights and free spanning pipelines, modeling only the warp line and warp line bracket interaction may be regarded as sufficient. However, for pipelines resting on the seabed and lower span heights a more complete definition of the clump weight geometry should be included.

Penetration of the pipeline and spurious pull-over behavior has been a reoccurring challenge in using SIMLA for simulating pull-over interference with free spanning pipelines, both for trawl doors and in this case clump weights. In general, as high normal contact stiffness is necessary to represent the outer pipeline geometry, the problem arises when contact is lost during interference and results in penetration of the pipeline. As contact again is obtained, due to the high stiffness, the pipeline and clump weight are violently pushed in opposite direction. To avoid this, it is recommended that a contact element arrangement defining a consistent search area during interference is applied, as described in Section 4.4.

As depicted in Section 4.4.1 , the simulations proved insensitive to the applied contact friction between the clump weight and pipeline. Friction properties were activated prior to interference and the friction coefficient was varied between 0.0 and 0.8 without any influence on the simulation result. Thus, the simulations have to be regarded as carried out without the effect of friction. Various measures was however tried in order to include friction. Experimenting with both contact and isocontact properties and a shorter rise time of the interaction curve defining the friction coefficient proved unsuccessful. The source of this problem was not accounted for. However, compared to the experimental test results, the influence of friction proved less significant for the simulations scenarios considered. Simulation of higher free spans were the warp line will slide a longer distance along the pipeline prior to impact, and for lower free spans were a more uniform sliding motion of the clump weight may occur, friction may be of greater influence. How to include friction in this case should thus be investigated further.

The effect of pipeline flexibility and corresponding reduction of pull-over loads should be investigated further. All simulations were in this case carried out for a 12” pipeline and a single trawling configuration with respect to clump weight mass and trawling velocity. More simulations varying the pipeline stiffness should be carried out for different span height, pipeline diameter, clump weight mass and trawling velocity in order to increase the knowledge of how pipeline flexibility influences the pull-over loads. This may again provide a basis for developing a simplified analysis procedure in pipeline design i.e. the effect of pipeline flexibility may for instance be incorporated into current calculation procedures by a reduction factor or an iterative process dependent on the induced pipeline displacements during pull-over, which is the case for calculation of pull-over duration in current engineering practice.

References

[1] Hagbart S. Alsos. *PhD. Trial Lecture: Analysis and Design of Subsea Pipelines Subjected to High Temperature and High Pressure*. Department of Marine Technology, NTNU, 2008.

[2] Robert D. Cook, David S. Malkus, Michael E. Plesha, and Robert J. Witt. *Concepts and Application of Finite Element Analysis, 4th edition*. John Wiley and Sons, INC., 2001.

[3] DNV. *Recomended Practice DNV-RP-F111, Interference Between Trawl Gear and Pipelines*. DNV, Høvik, Norway, 2006.

[4] DNV. *Offshore Standard DNV-OS-F101, Submarine Pipeline Systems*. DNV, Høvik, Norway, 2007.

[5] Anders Endal and Harald Ellingsen. *Lecture notes: TMR 4135 - Fishing Vessels and Workboats, Chapter 2, Fishing Technology*. Department of Marine Technology, NTNU, 2007.

[6] O.M. Faltinsen. *Sea Loads on Ships and Offshore Structures*. Cambridge University Press, 1990.

[7] Olav Fyrileiv, Dag Ø. Askheim, Richard Verley, and Hanne Rolsdorph. Pipeline-trawl interaction: Effect of trawl clump weights. *OMAE2006-92128*, 2006.

[8] Ragnar T. Igland and Tore Søreide. *Advanced Pipeline Trawl Gear Impact Design*. Reinertsen Engineering, Trondheim, Norway, 2008.

[9] Ludvig Karlsen. *Redskapsteknologi i fiske*. Universitetsforlaget, 1989.

[10] Ludvig Karlsen. *Redskapslære og fangstteknologi*. Landbruksforlaget, 1997.

[11] Ivar Langen and Ragnar Sigbjörnsson. *Dynamisk analyse av konstruksjoner*. Tapir, 1979.

[12] Vegard Longva. *Simulation of Trawl Loads on Subsea Pipelines*. MSc Thesis NTNU, Department of Marine Technology, Trondheim, 2010.

[13] Vegard Longva, Svein Sævik, Erik Levold, Håvar Ilstad, and Per Teigen. *Dynamic Simulation of Free-Spanning Pipeline Trawl Board Pull-over,Proceedings of the 30th International Conference on Ocean, Offshore and Arctic Engineering, OMAE2011-49592*. ASME, 2011.

[14] Martin Troels Møller. *Simulation of Interference between Trawl Gear and Pipelines*. MSc Thesis NTNU, Department of Structural Engineering, Trondheim, 2009.

[15] Torgeir Moan. *TMR 4190 - Finite Element Modeling and Analysis of Marine Structures*. Department of Marine Technology, NTNU, 2003.

[16] Ivar Nygaard. *Kristin and Snøhvit Pipelines in Free Spans. Overtrawling by Clump Weights. Model Tests*. MARINTEK, Trondheim, Norway, 2004.

[17] Svein Sævik. *SIMLA - Theory Manual*. MARINTEK, Trondheim, Norway, 2008.

[18] Svein Sævik, Ole David Økland, Gro Sagli Baarholm, and Janne K.Ø. Gjøsteen. *SIMLA Version 3.15.0 User Manual)*. MARINTEK, Trondheim, Norway, 2010.

Appendix A

Thyborøn Roller Type Clump Weight

This appendix includes drawings of a Thyborøn roller type clump weight, which were supplied from manufacturer to this thesis work. The cross-section properties of the clump weight applied in the simulations have been taken form this drawing. The drawing is however for a larger clump weight than modeled, which was 2.67 m in total and initially 3840kg before ballasted to 6100 kg. However, according to manufacturer the cross-section is in general not changed for different sizes of roller type clump weights. Only the roller length and wall thickness are changed.

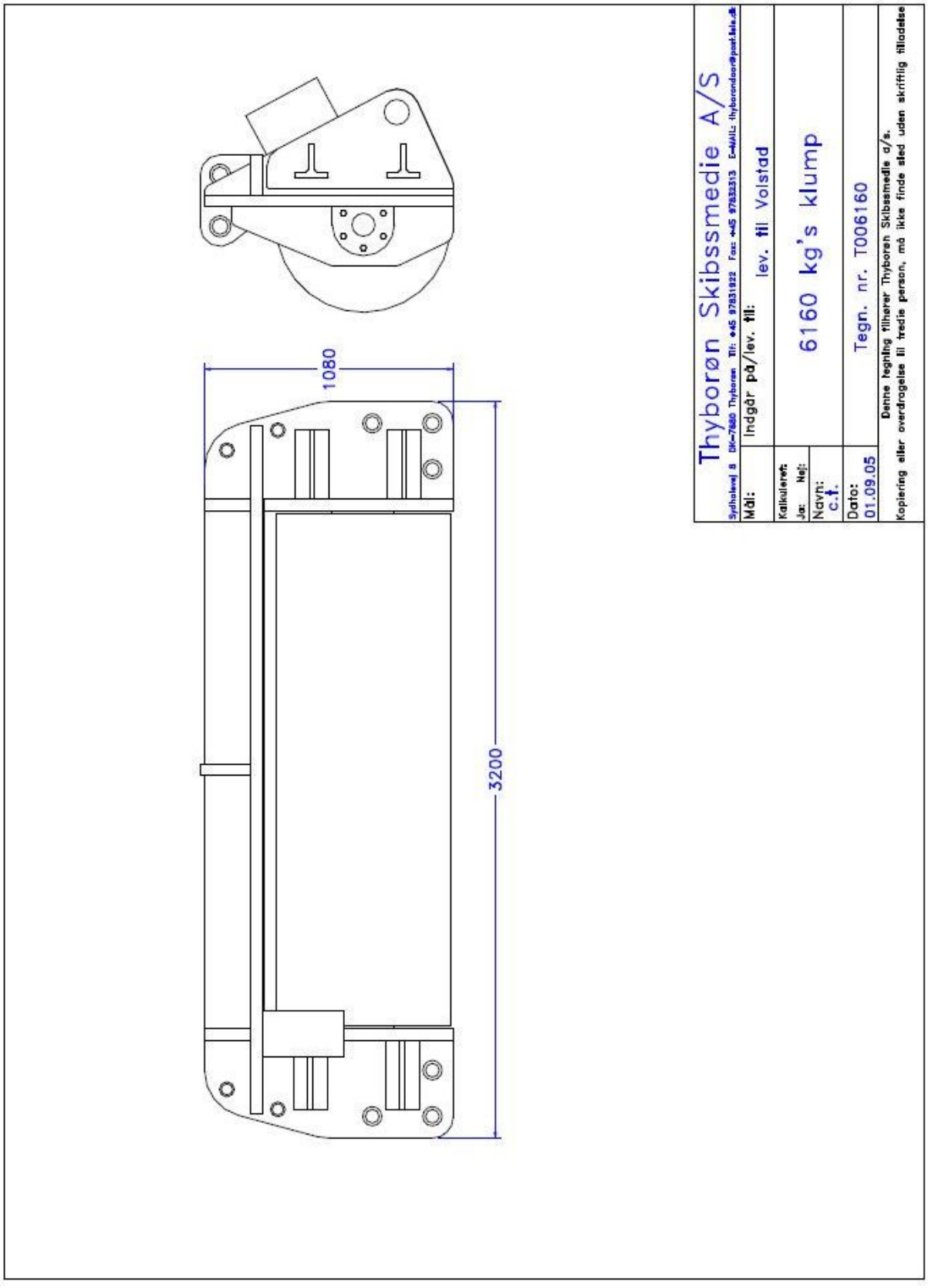
1080
3200
Thyborøn Skibssmedie A/S
Sydhavnvej 8 DK-7680 Thyborøn Tlf: +45 97831022 Fax: +45 97832313 E-MAIL: thybornsmed@post.tele.dk
Mål:
Indgår på/lev. til:
lev. til Volstad
Kalkuleret:
Ja: Nej:
Navn:
c.t.
6160 kg's klump
Dato:
01.09.05
Tegn. nr. T006160
Denne tegning tilhører Thyborøn Skibssmedie a/s.
Kopiering eller overdragelse til tredie person, må ikke finde sted uden skriftlig tilladelse

Appendix B

Additional Clump Weight Data

Specific dimensions and mass distribution of the model scale clump weight used in the experimental tests was initially not clear from the MARINTEK report [16]. Measurements of a similar scale model were obtained from SINTEF Fisheries and Aquaculture, Hirtshals, Denmark. Two illustrations and clump weight properties of this model are included in this appendix.

Quantity	**Symbol**	**Value**	**Unit**
Total length	l_t	2.67	m
Roller diameter	D_r	0.76	m
Roller length	l_r	1.55	m
Total dry weight	m_t	3840	kg
Ballast weights	m_b	1000	kg
Weight of frame	m_f	1400	kg
Wight of roller	m_r	1420	kg

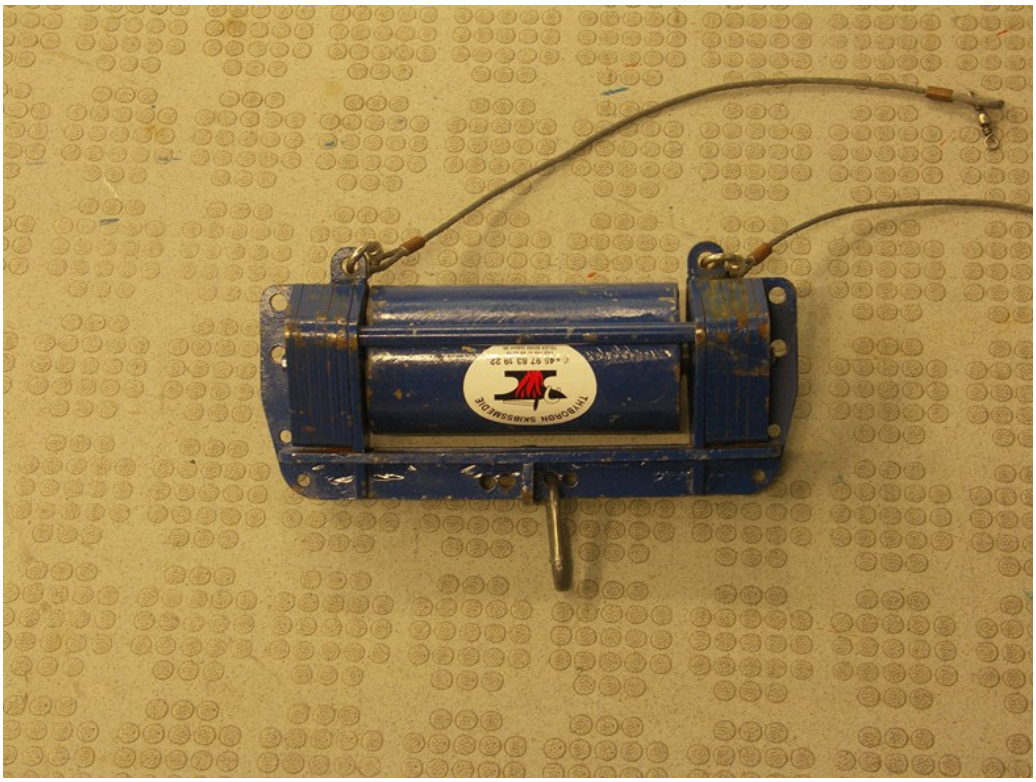

Figure B.1: SINTEF Thyborøn clump weight model

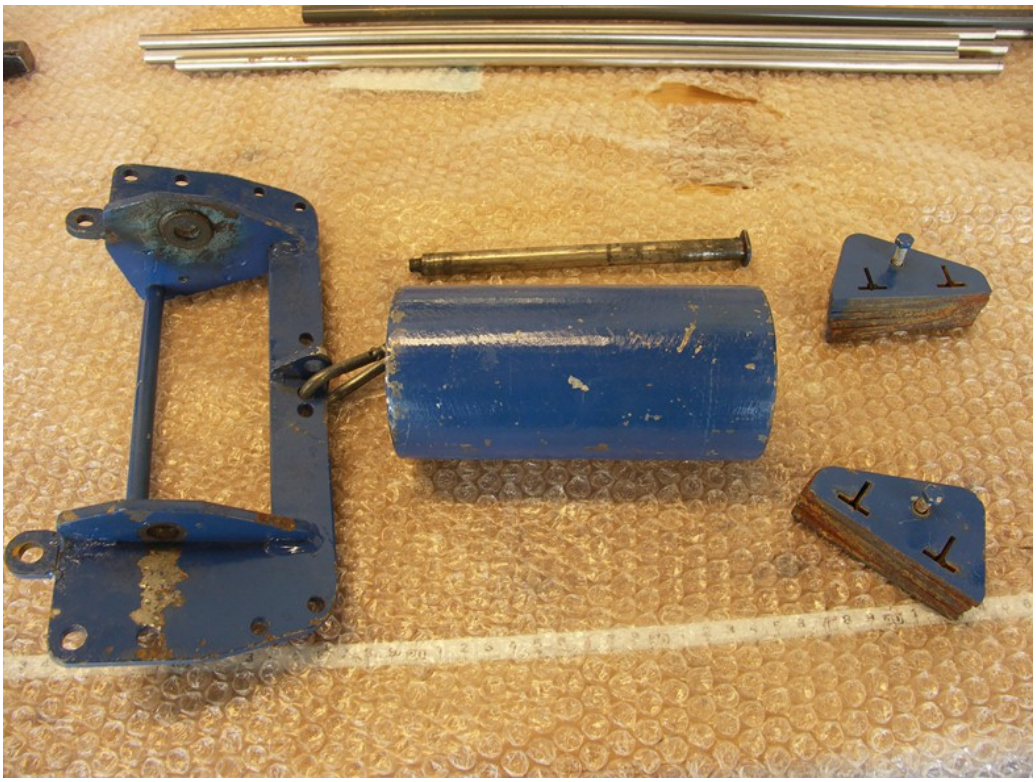

Figure B.2: SINTEF Thyborøn clump weight model

Appendix C

Contact Problem

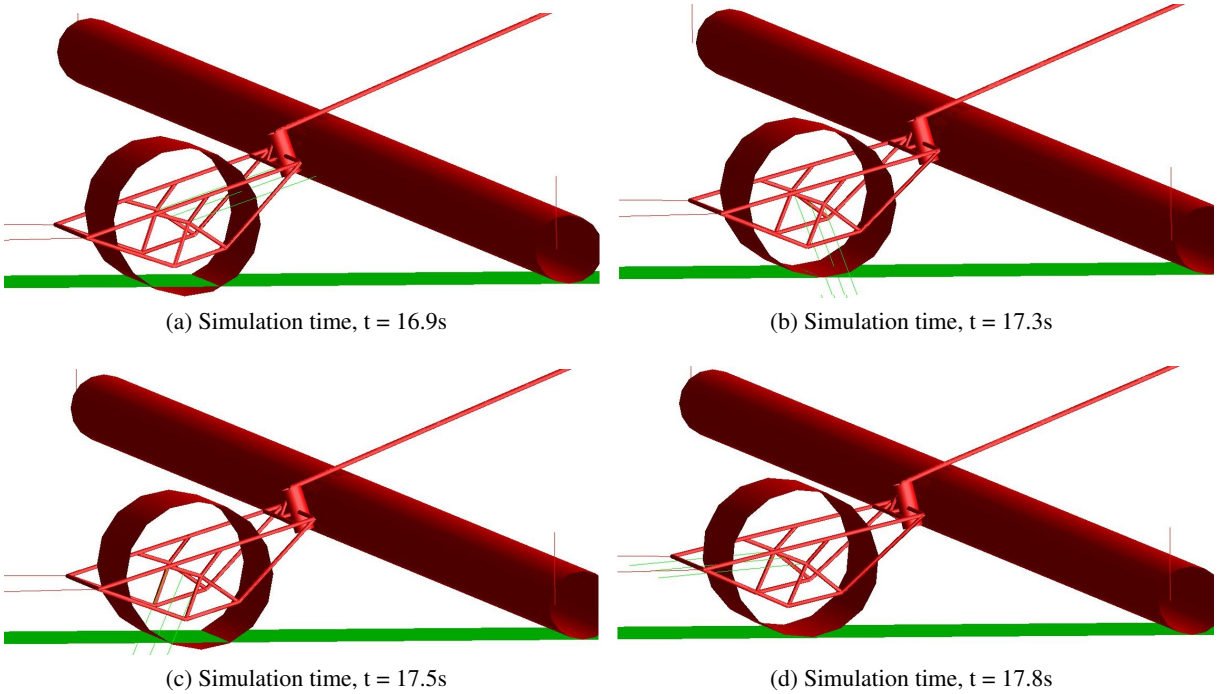

(a) Simulation time, t = 16.9s

(b) Simulation time, t = 17.3s

(c) Simulation time, t = 17.5s

(d) Simulation time, t = 17.8s

Figure C.1: Illustration of contact problem due to high contact stiffness applied both to the seabed and pipeline.

Appendix D

Complete Set of Contact Interfaces

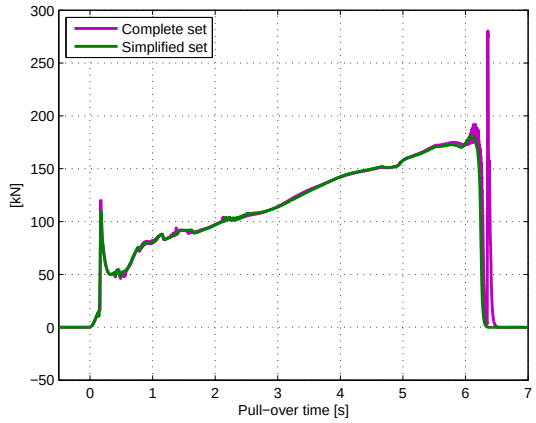

(a) Horizontal pull-over force

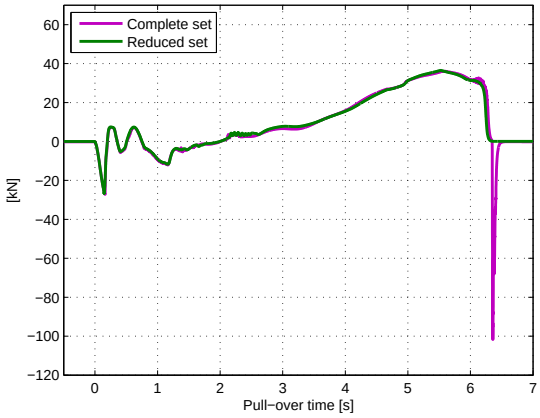

(b) Vertical pull-over force

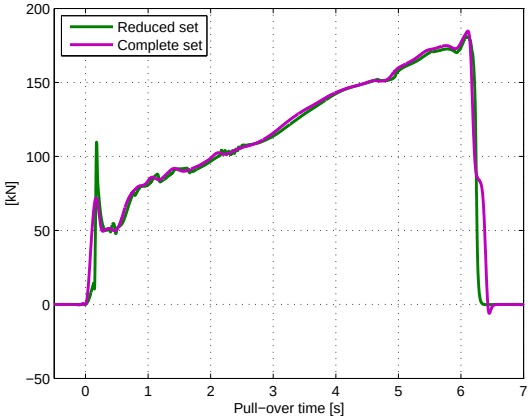

(c) Filtered horizontal pull-over force

Figure D.1: Pull-over forces applying a complete set of contact interfaces. The simulation was carried out with the free spanning pipeline model for a span height of 0.5 m.

Appendix E

Average Filtering of Simulation Results

A moving average filter was in some cases applied to the pull-over forces in order to reduce interfering oscillations in the plots. For comparison the force-time histories for unfiltered and filtered values are given in this appendix.

The simulation results with the experimental test model for a span height of 0.25 m have been filtered to remove what is believed to be eigenfrequency oscillations from the warp line bracket to pipeline interaction. The eigenperiod for this interaction was calculated to about 0.1 s.

All horizontal and vertical pull-over forces from the free spanning pipeline model have been filtered to remove high frequency oscillations. The oscillations occur close to maximum horizontal force and are believed caused by temporary loss of contact as the lower edge of the warp line bracket slides over the pipeline.

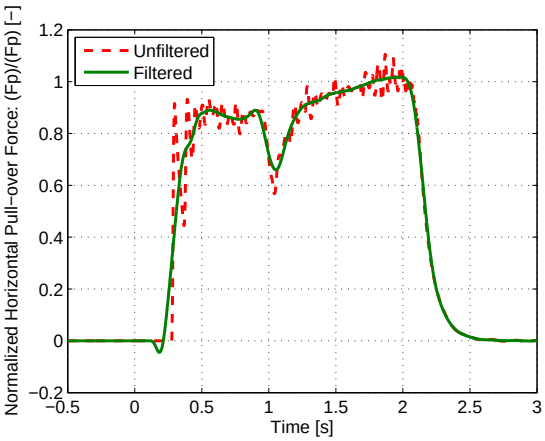

(a) Test no. 3100 - Flexible

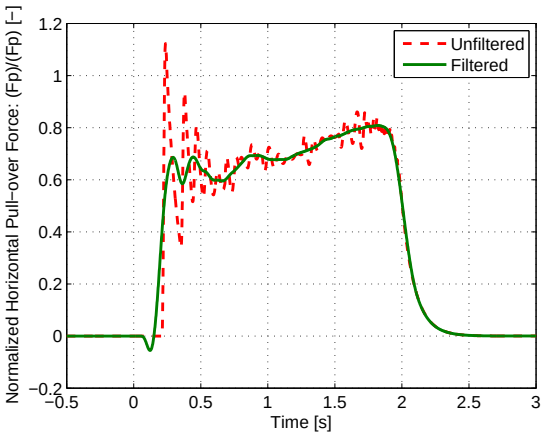

(b) Test no. 3120 - Fixed

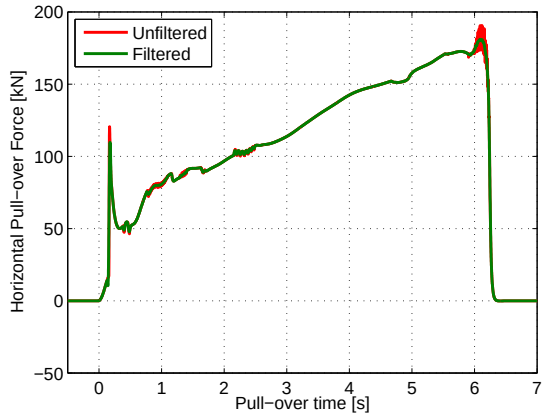

(c) Free spanning pipeline model - 0.5 m

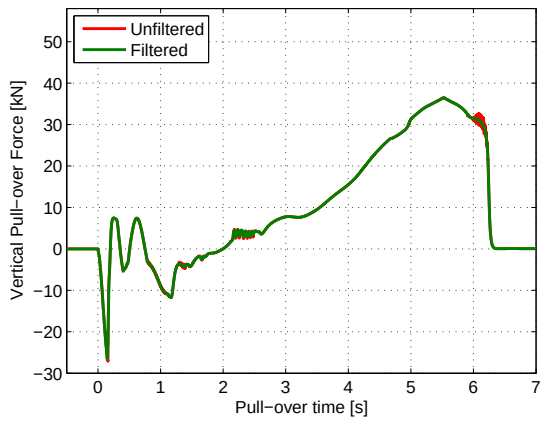

(d) Free spanning pipeline model - 0.5 m

Figure E.1: Filtered relative to unfiltered pull-over forces

Appendix F

Lower Warp Line Attachment Point

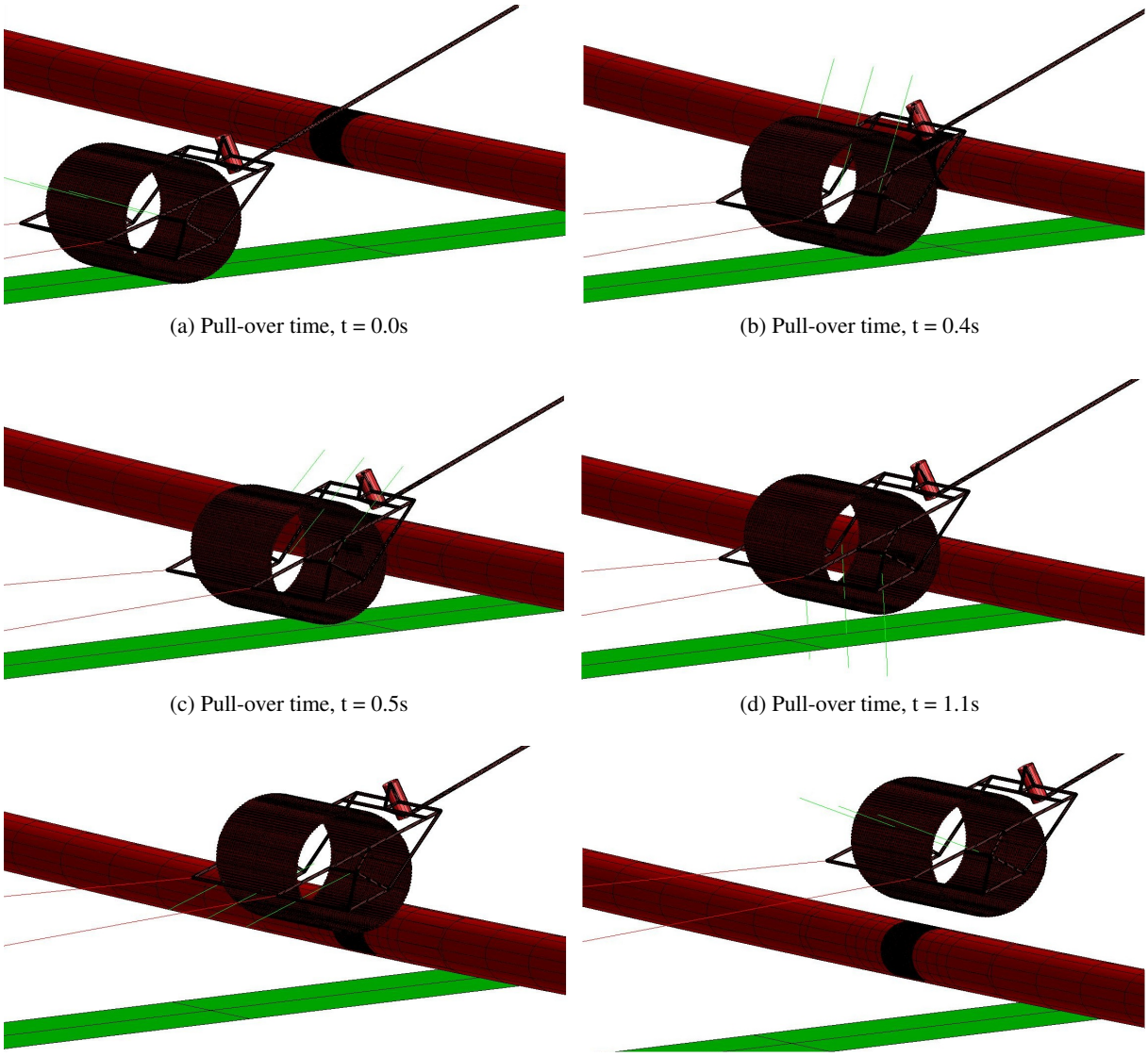

(a) Pull-over time, t = 0.0s

(b) Pull-over time, t = 0.4s

(c) Pull-over time, t = 0.5s

(d) Pull-over time, t = 1.1s

(e) Pull-over time, t = 1.4s

(f) Pull-over time, t = 1.6s

Figure F.1: Screen shots from simulating a lower warp line attachment point for a span height of 0.5 m with the free spanning pipeline model. The extension of the seabed is removed for illustration purposes.